European Research Infrastructure supporting Smart Grid Systems Technology Development, Validation and Roll Out

Technical Report TA User Project

Locally Manufactured Small Wind Turbines for Rural Electrification in Nepal

Document Information

Document Version: 4

Revision / Status: Final

All Authors/Partners: Kimon Silwal (KAPEG), Rojesh Dahal (KAPEG), Sean Paul (Nelson Mandela Metropolitan University), Kostas Latoufis (ICCS-NTUA)

Distribution List

Document History

Revision	Content / Changes	Resp. Partner	Date
[Rev. 1]	Evaluation of data, calculations, methodology chapter, analysis chapter and introductions and conclusions	Kimon Silwal (KAPEG)	27.02.2019
[Rev. 2]	Second version, including overall draft report review and comments	Kimon Silwal (KAPEG), Kostas Latoufis (ICCS-NTUA)	05.08.2019
[Rev. 3]	Updating the commented sections	Kimon Silwal (KAPEG)	10.09.2019
[Rev. 4]	Final review and completion	Kimon Silwal (KAPEG), Kostas Latoufis (ICCS-NTUA)	18.09.2019

Document Approval

Final Approval	Name	Resp. Partner	Date
Final Approval	Kostas Latoufis	ICCS-NTUA	18.09.2019

Disclaimer

Copyright Notice

TABLE OF CONTENTS

Abbreviations

SWT: Small Wind Turbine

KAPEG: Kathmandu Alternative Power and Energy Group

AFPMG: Axial Flux Permanent Magnet Generator

MHP: Micro-hydro Plant

AEPC: Alternative Energy Promotion Centre

EESL: Electrical Energy Systems Laboratory

ICCS: Institute of Communications and Computer Systems

NTUA: National Technical University of Athens

EES: Electrical Energy System

O&M: Operation and Maintenance

Cp: Aerodynamic Coefficient

TSR: Tip Speed Ratio

ARP: Access Responsible Person

List of Figures

List of Tables

Executive Summary

This research tested the performance of AFPM generator and a small wind turbine at ICCS-NTUA lab and Rafina SWT test site (Meltemi) in Greece. The locally constructed SWT was constructed at KAPEG and shipped to Greece where the AFPMG was tested for seven days and the SWT taken to test site for installation. The results from the bench testing and the test site is compared with the OpenAFPM simulation tool, which was used to the design the AFPMG in the beginning by the lead users.

Previous experiences have shown that although the wind potential exists in specific regions of Nepal, the technical issues with the locally constructed SWT's has been one of the constraining factors for further technology implementation. These technical issues arise in the form of available permanents magnets, copper wires and bearings and other mechanical parts. KAPEG with its work of SWT's in the last decade, therefore, wants to test the locally fabricated system to investigate the performance of its locally built SWT's and upscale the field implementation works further in the coming future, the first part of which has been successfully carried out through the TA project.

The online simulation tool is made to assist small wind turbine practitioners and researchers around the world. Therefore, the lead users worked in close coordination with the ARP long before the project started to ensure the AFPMG is designed and constructed through the standard design process and finally its validation carried out through the test's facilities at NTUA.

The plots from the OpenAFPM simulation tool used for designing the AFPMG tested is compared with the actual measurements extracted from the bench testing results.

There is a close resemblance between the torque-speed characteristics of the simulation results and the test bench results. The mechanical torque calculated by adding the losses (friction, windage and copper) best matches the simulation results with a percentage error of 1%. The mechanical torque taken from the direct measurements from the torque meter compared with the simulation results give the percentage error of 17%. From the test results, there is a clear indication that the calculated results with adding losses technique significantly matches the simulation. With close similarity between the torque relationship between the simulation and the adding losses approach, the results plotted and compared for electrical and mechanical power also is very close to one another.

The mechanical power calculated using torquemeter incorporates slightly more losses than the one with adding losses. The direct effect on the efficiency calculated from these two approaches is observed, as seen in Figure 28. The difference of 12% of peak efficiency is observed from the two approaches of calculating mechanical power.

The rotational loss (friction and windage) of 20W is calculated at the maximum allowable shaft speed in the test bench of 720rpm. The copper losses observed between the simulation and the test bench results are comfortably close to the simulation results. The apparent difference of the copper loss between the simulation and the test bench could be arising from the slight difference in phase resistance.

The data logger was used to measure the performance of the 200W neodymium AFPM generator that was previously tested in the laboratory, whilst in normal operation as part of a battery

connected wind power system installed at the test site according to the international standard *IEC 61400-12-1*. Peak power was measured to be 162W at 12m/s, above which the furling system causes power production to drop to protect the turbine from dangerously high winds. The maximum efficiency of 0.23 is reached at 6m/s, while at the rated wind speed of 10m/s, the system efficiency drops to 0.2 due to the action of the furling system. On a site with 5m/s mean wind speed, the SWT would be expected to produce 276kWh/year. The cut-in speed with a battery was found to be 359rpm at 3m/s. This closely matches the simulation design where the system cuts in at 3.2m/s with the rotational speed of the turbine at 348rpm.

Parameters	Open AFPM Simulation Tool	Field Test Results
Cut – in wind speed	3m/s	3.2m/s
Cut - rpm	348rpm	357
Rpm at nominal wind speed	607rpm	650rpm
Power at nominal wind speed	200W	217W
Nominal TSR	3	3.5
Cp peak	0.2	0.23

The correlation between the design tool and the actual measurements carried out through the TA project will primarily be useful to construct the future AFPMG machines of different capacities at KAPEG office with the flexibility in using a range of permanent magnets, copper wires and other similar SWT components.

1. General Information of the User Project

User Project Title: Locally Manufactured Small Wind Turbines for Rural Electrification in Nepal

User Project Acronym: LMSWT-Nepal

Host Infrastructure: ICCS-NTUA

Start date – End date: 27/10/2018 – 10/11/2018

User Group Members: Kimon Silwal, Rojesh Dahal, Sean Paul

2. Research Motivation

Kathmandu Alternative Power and Energy Group (KAPEG) in Nepal have been working on a small wind turbine system (SWT) since 2004. It is a research and development-oriented firm working in the field of the renewable energy sector in Nepal. Initially, the work in the field of SWT started with the selection and mechanical testing of timber materials available in Nepal most suitable for SWT blade construction in partnership with Riso-DTU [1][2][3]. The research and development work since then has been a continuous effort to build efficient SWT with locally available materials and resources in context to the Nepalese geographical terrain and its wind patterns.

The results obtained from a project carried out in 2011 for developing commercially viable wind turbine system identified the necessity to redesign the AFPMG to match the performance of the original KAPEG SWT design. In the absence of the standard bench testing and field-testing facility, the SWT work at KAPEG continued with the aim to build established designs available to achieve the goal of basic energy access for rural community electrification.

Piggott's [4] A Wind Turbine Recipe Book gives a step by step guide for manufacturing a range of SWTs (Small Wind Turbines) from 1.2 - 4.2m rotor diameter using only basic tools and techniques and readily available materials. The open-source Piggot's design was implemented later using locally available materials at the field for performance validation to make it fit for community electrification.

Although the construction recipe book contains the detail process of SWT manufacturing, the locally available resources and components differs in different parts of the world. The availability of materials is more difficult specially in the developing nation like Nepal. The variations of resources like permanent magnets, copper wires, timber material, iron materials and bearing hub during the construction of the small wind turbine exists in most extent. KAPEG has experiences of component variations in terms of availability, especially for permanent magnets, bearing hubs and copper wires compared to the recipe book. Generally, the variations in specifications of permanent magnets and copper wires can lead to performance changes.

Figure 1: Different types of wheel hub bearing used for the small wind turbine

Trailer Hub   Small car wheel hub

The use of a trailer hub is seen to be more frequent than the small car wheel hubs in the most of the cases with locally constructed SWT's. The reason is that the trailer hub comes with a standard set of the shaft and with a proper hub locking mechanism which is more facile during the construction. The trailer hub contains a tapered bearing. The bearing hub used by KAPEG is the small car wheel hub, which is easier to find and uses the roller type bearing. The difference may be

minimal in terms of performance but care needs to be taken in terms of mechanical robustness. A certain degree of variation exists in available sizes of copper wire influencing the size of the stator and perhaps the electrical characteristics of the machine.

The prior assessment has shown that most of the locally constructed small wind turbines installed in the past by different practitioners in Nepal have been investigated to have technical issues. The implementation of the small wind systems is Piggot's designs. One of the key technical issues is the permanent magnets used during the wind turbine construction process leading to poor system performance. The experience has shown that procuring small batch of magnets from China and India does not comply with the required specification.

The online tool called openAFPM developed by the Rural Electrification Research Group (RurERG), which is part of the Smart RUE (Smart grids Research Unit of the Electrical and Computer Engineering School) of the National Technical University of Athens (NTUA) is used to design and construct the small wind turbine with the use of locally available materials at KAPEG. The tool gives larger range of flexibility to design the SWT's in accordance to the local resource availability mainly with type of the magnetic material and the copper wires.

The TA project provided a more exceptional opportunity for learning and testing as the design and testing both were supervised by the online design tool developer. The tests carried out through this project for the SWT build by KAPEG with the use of online design tool is the primary motivation such that the turbine capacities can be upscaled with the use of local materials maintaining the optimal performances.

2.1. Objectives

Laboratory testing:

- Bench testing AFPMG built by KAPEG to characterize its performance.

Field Testing:

- Conducting field test at the test site for the 1.2m rotor blades to generate the performance of the SWT.

The experiments are designed to provide in-depth knowledge of the system and so that the results can be used for further improvements.

2.2. Scope

KAPEG has been working in the field of small wind turbines in the last decade being involved in various local and international scale projects for product, capacity and various feasibility studies. The locally constructed SWT's at KAPEG has never been tested in the standard lab facilities before. The proposed transnational access project seeks to bring the KAPEG built 1.2m locally constructed small wind turbine with the generator designed through OpenAFPM simulation tool into rigorous tests and measurements. The small wind testing facilities at the ICCS-NTUA lab and its IEC standard test site in Rafina is used to perform various tests and collect measurements for analysis.

The lab tests refer to bench testing the AFPMG. The results of the AFPMG testing at various operating conditions will assist the future simulations, modeling, and local construction. The performance of the SWT at the test site will identify the critical performance of the machine.

The project is to bring technical confidence to KAPEG in terms of system performance while being able to improve the service and maintenance, which is continuously required by SWT systems technology.

3. State-of-the-Art/State-of-Technology

Nepal is a landlocked country with 2/3rd of the country's area occupied by the Himalayas and mountainous terrain. Consequently, a large population in Nepal have historically met their energy needs from biomass, imported kerosene, and traditional water-powered mills [5]. According to the 2017 Global Tracking Framework release, Nepal has access to electricity rate of 91%, with urban and rural access rates of 85% and 95% respectively [6]. The increase in electricity access between 2010 and 2016 has also seen rises over 2% growth annually. This growth is primarily due to increased levels of connections to the National Grid, but also through off-grid Micro-Hydropower (MHP) and solar projects. To date, there are only a relatively small number of Wind Turbine installations in Nepal. Although the access to electricity is increasing in the rural areas in Nepal, the quality and quantity of the electricity supply are highly erratic [7]. The electricity access binary is potentially misleading despite the significant increases in electrification rates over recent years, as evidenced by the increased use of the multi-tier framework (MTF) by energy practitioners when considering electricity access. Many households considered as having electricity access may only have access to a solar lantern or pico-solar home system, or otherwise intermittent and unreliable access which has limited impact on the potential for economic growth, individual empowerment, and participation in the broader Nepali society. Continued efforts are required to provide rural populations with reliable and cost-effective electricity access to enable sustainable growth. Therefore, the government of Nepal has placed significant importance to energy security with a diverse energy mix as a forefront strategy for energy access, especially for the rural population.

As one of the world's most mountainous countries, grid extension in Nepal is economically unfeasible in many locations. As a result, off-grid electrification solutions will be required to provide or upgrade access to electricity in the most inaccessible regions of Nepal.

In 1989, two 10kW wind turbines, combined with battery storage, were installed in Kagbeni, Mustang District. Within three months of installation, the turbines were catastrophically damaged by strong winds, effectively ending the first significant wind installation project in the country. This unfortunate incident has negatively affected the mainstream perception of wind technology in the country and may have significantly delayed the development of the wind power sector in the country, whilst other technologies continued their development to present day. Since 1989 the design and manufacturing processes of wind turbines has made significant progress. Since the ill-fated project in Kagbeni, several other wind installations have been made. Between 2002 and 2007 Practical Action Nepal installed several locally manufactured small wind turbines, ranging from 200W to 1kW in size, across the country. The potential cause of many projects being non-operational may be due to lack of maintenance and other technical problems.

Figure 2: Stand-alone small wind turbine installed in the location called Phakhel in central development region of the country for providing electricity for a primary school. The system stopped operating within few months due to several technical issues.

With reference to previous assessments, demonstration of SWT's in Nepal has faced significant obstacles with system technology being one of the principal factors. With installations of more than 15 SWT's in coordination from local manufacturers by Practical Action Nepal, most of the installations ceased to operate in a short period while one of the primary reasons for the system failures being unverified power performance and inadequate testing for the locally constructed wind turbines. The demonstration projects for locally built small wind have remained mostly ineffective in the last decade [3]. Several projects have been conducted to demonstrate the viability of locally constructed small wind turbines in Nepal. Lack of technical expertise and resources creates more significant challenges for technology. The higher possibility of the system being inefficient added to the intricate weather conditions and complex terrain increases more difficulties [3]. The influx of Chinese wind turbines into Nepal creates increased cost and challenges to provide proper O&M [8]. The imported technology does not consider the uneven terrain and higher altitude affecting the annual energy yield. The commercial system faces higher capital cost during procurement with doubtful performance curves. Small wind turbines in the hybrid mix with the photovoltaic system in recent years are becoming more relevant and suited to off-grid community electrification for basic access to electricity.

As a part of the national energy mix strategy, wind energy is considered as a potential resource in a strategical point of view. More recently, the AEPC, in partnership with the ADB, has been implementing solar/wind hybrid mini-grids in off-grid communities [9]. KAPEG conducted a site survey of the wind-solar hybrid systems in six installations sites across the country, producing results of complex technical issues associated with the commercial turbines [10].

KAPEG is one of the few practitioners continuing its research and development in the field of small wind turbines in Nepal since 2003 to meet the energy needs in windy areas where the grid connection is not possible. An economically viable, robust and sustainable system requires the use of locally available materials, simple technology, and workforce. Therefore, KAPEG has been working to develop turbine blades with locally available timber materials while studying their mechanical properties, such as fatigue life, static properties, weathering life, hardness, fracture, toughness, etc. [1] [2]. Generally, the wooden blades are hand carved with the aid of bottom and top templates such that the aerodynamic profile meets the design consistency throughout the various sections of the blade. It is observed from previous projects that no significant flaws are found in blade profiles in regards to the handmade construction of blades [3]. The Piggott's design of AFPMG has been utilized in the past using locally available materials with some variations in the mechanical system design by KAPEG.

Figure 3 shows the recent installation of a small wind turbine in the mid-western part of the country in an off-grid village of Mityal implemented by KAPEG. The system is the hybridization between the 2.4m diameter locally built wind turbine and 600W photovoltaic system powering the village administrative office and the local health post to fulfil the basic electricity needs.

Figure 3: Picture of the most recent installation of a solar wind hybrid system by KAPEG at the remote offgrid village of Mityal in mid-western part of the country.

The technique locally adapted is the vehicle testing procedure (VTP) to test the performance of the SWT's constructed by KAPEG in the past [11] [12]. Although the VTP is a quick way to check the performance of the wind turbine, KAPEG has not yet validated the testing procedure. Also, the

challenges faced during a VTP are significant. More in-depth tests separately for the AFPMG in the test bench and the field test of the turbine is required to compare the results.

The testing of AFPMG in the test bench at ICCS-NTUA will produce an accurate model of the turbine while the test site of SWT will create results identifying the overall performance of the turbine pinpointing areas of designs and construction which can be further improved.

Therefore, the project provided a perfect platform for the KAPEG constructed SWT's to validate its performance while enhancing its capacity to produce technically robust and efficient wind energy systems. The results of the constructed AFPMG model and turbine performance charts will extend the SWT frontier in Nepal as KAPEG strives to continue working with the SWT's in different areas of products and services, education, delivery model and developing contextual technical standard and guidelines.

4. System Description

The locally constructed SWT following the Piggot's design have the turbine blades carved from wood, the main bearing used from the trailer hub and much of the steelwork used from pieces of metal. Figure 4 shows an exploded view of the main components and sub-systems that make up a locally manufactured wind turbine. Figure 5 shows the fabrication of stator and rotor components of the axial permanent magnet generator as illustrated in the exploded view of Figure 1.

Figure 4: (Image left) Exploded view of the rotor and stator discs that make up an AFPM generator; (Image right) The magnetic field created by the permanent magnets and steel rotor discs
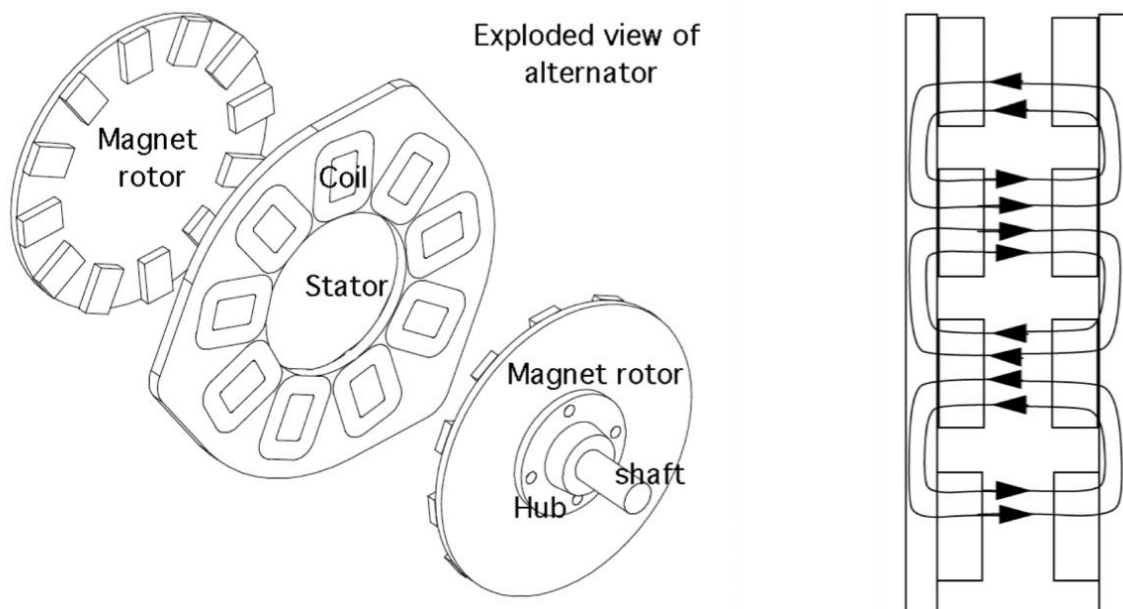
The Axial Flux Permanent Magnet (AFPM) generator sits at the heart of this small wind turbine, converting the rotational energy from the blades into 3-phase electrical power to charge a battery bank and ultimately provide the energy services such as electric lighting, mobile phone charging and vaccine refrigeration. Until now, the most frequently used permanent magnet (PM) generator topology for wind turbine applications has been radial flux. Whilst this is still common practice in large wind turbines, the use of permanent magnets in a coreless axial flux generator simplifies the construction process due to absence of excitation windings (which also makes the machine more efficient and more compact) and by using only planar components. In addition, the ability to place a large number of pole pairs in the rotor of the generator, makes the use of a gearbox unnecessary, a component that is expensive and in need of frequent maintenance.

Figure 5: Picturing showing the various stages of the small wind turbine construction processes.

The Figure 5 shows the various phases of the construction during the wind turbine building process. Figure 5 demonstrates an example of the 4.2m diameter SWT constructed by KAPEG.

AFPM generators are a branch of 'non-excited' synchronous generators, consisting of three main parts: two rotating steel disks, carrying permanent magnets and one steady stator, carrying the coils of copper wire. The magnets are permanently excited, i.e. they carry a constant magnetic field. The coils are star- connected to a 3-phase system. The rotational movement of the magnet disks induces voltage and current into the stator.

The advantages of synchronous generators excited by permanent rather than electro-magnets are:

- No additional power source is required for the excitation of the rotating coils.
- No brushes and slip-rings are needed for the electrical connection of the electro-magnets.

The disadvantages are:

- The magnetic excitation field is constant and cannot be regulated in order to influence the performance of the generator, i.e.to maximise its overall efficiency.
- The mining of raw earths such as Neodymium (Nd), which is needed to produce strong enough permanent magnets, entails particularly severe environmental damage and contamination.

AFPM generators need to be designed and constructed in a very precise way in order to do their job properly.

- The magnetic field in between the coils must be as strong as possible: small air gap, strong magnets (high field) and thick iron disks in order to close the magnetic circuits towards the back.
- The heat losses in the coil wires must be minimal: thick wire section, little air between the windings (good quality winding), good heat evacuation on the surface of stator.
- The relation between the magnet-poles (number of magnets) to stator-coils must allow for the required phase difference of 120° between the three voltage curves, i.e. for 3- phase AC production.
- The magnetic pole-pairs as well as the rotational speed (rpm) of the moving parts must result in exactly the range of voltage needed to either charge a battery system or to feed electricity into the grid: the number of coil-windings must be calculated accordingly.

4.1. Technical specification of the Small Wind Turbine System

Table 1: SWT specification table – This is the SWT tested at lab and at test site

Components	Value	Figure 6: Picture of the SWT turbine under test
Blade		
Turbine Radius	0.6m	
Design CP	0.2	
Design Cut-in Wind Speed	3m/s	
Nominal Wind Speed	12m/s	
Cut-in TSR	6.25	
Design TSR	3	
Mechanical Power at nominal wind speed	228W	

Figure 6: Picture of the SWT turbine under test

Generator			
Nominal Voltage	12V	Winding configuration	Series
Rated DC power at nominal speed	200W	Phase configuration	Star
Number of coils turn	73	Line out	Three terminals without neutral
Number of coils	6	Design cut-in RPM	348
Copper wire thickness	1.5	Rotor disc diameter	242mm
Number of poles	8	Rotor disc thickness	8mm
Air gap (between magnets)	23	Magnetic Material	NdFeB N40
Magnet's Length, Width and Thickness	30mm*46mm*10mm		
Other information			
Cost of the SWT	80,000 NPR		
Total Weight SWT	22kg		

The above specification was used as input in the openAFPM tool [13] to compare the results of the simulation and the actual results obtained from the bench testing in the ICCS-NTUA lab. The next section of the report provides a further description of the tool.

5. **Methodology**

5.1. OpenAFPM

OpenAFPM an open-source software tool for modeling and designing AFPM generators in electric wind systems [12]. The OpenAFPM modeling tools can be used for designing Axial Flux Permanent Magnet (AFPM) generators for wind electric systems with the use of the open source finite element analysis software 'Finite Element Method Magnetics' (FEMM). This series of design tools have been developed by the Rural Electrification Research Group (RurERG,), which is part of the Smart RUE (Smart grids Research Unit of the Electrical and Computer Engineering School) of the National Technical University of Athens (NTUA), in order to assist designers and practitioners involved with small scale wind electric systems.

The OpenAFPM tools series consists of three design tools named MagnAFPM, UserAFPM and OptiAFPM. The tool MagnAFPM can be used for designing a generator for a specific set of rotor blades and a specific set of permanent magnet dimensions. The tool UserAFPM can be used to validate the performance of a particular generator geometry by performing a finite element analysis using FEMM. The tool OptiAFPM uses the particle swarm optimization (PSO) to optimize the dimensions of the permanent magnets used in the generator design for a specific set of rotor blades, while minimizing the generator's cost and mass, and maximizing its efficiency.

The Access Responsible Person (ARP) of the TA project Access provider ICCS-NTUA is the developer of the openAFPM simulation tool made to assist small wind turbine practitioners and researchers around the world. Therefore, the lead users worked in close coordination with the ARP long before the project started to ensure the AFPMG is designed and constructed through the standard design tool and for its validation carried out through the test's facilities at NTUA.

Over the next sections of the reports, the methodology for bench testing the AFPMG is described whose results are later compared with the simulation results from the openAFPM tool where possible. The comparison is mainly aimed for producing key differences such that the design tools can be later used to upscale the turbine construction using resources that may be variable in the local context such as permanent magnets and copper wires. The AFPMG is built using the online design tool and tested in the bench testing facilities at ICCS-NTUA with the supervision from the ARP while the entire SWT is put under test at the installation site to collect the measurements for generating different performance charts.

5.2. Bench Test Set-up and Experimental facility description

The experiments described in the subsequent section were performed in the Electrical Energy Systems Laboratory (EESL) laboratory of ICCS-NTUA. A TDE Macno speed drive and a 50HP low rpm Mawdsley's variable speed DC motor drive was used to drive the generator under test across a range of rotational speeds. The rotating shaft was mounted with a Datum 20Nm torque meter and chain couplings to allow for small misalignments in the shaft. To measure electrical data, a WT3000 precision power analyser was used to instantaneously measure and record three-phase voltages through high voltage AC probes and one line current through an AC/DC current sensor. A Terco ohmic resistive load of 3kW, split into three phases of 1kW each, was employed to create a constant load for the generator under battery load test across a range of operating conditions. An ACDelco

sealed maintenance free 90Ah-12V batteries and a 3-phase bridge rectifier were also used in later experiments to provide a load that more accurately represents the working conditions of an off-grid small wind turbine. The test bench shown in Figure 9 allows generators of various sizes to be coupled to the driving motor by providing both horizontal and vertical adjustment with the support of a central bearing. Further equipment that is specific to individual tests is introduced throughout the following section together with the methodology for that particular test.

Figure 7: Schematic of the test rig of the bench testing set-up
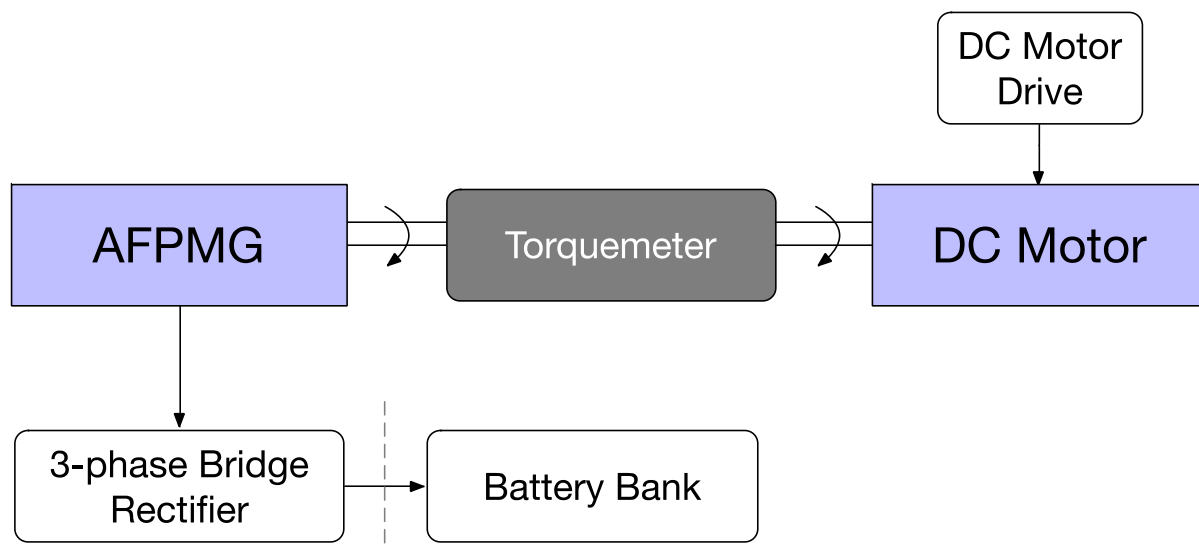
Figure 8: Picture of the measurement and test bench set-up
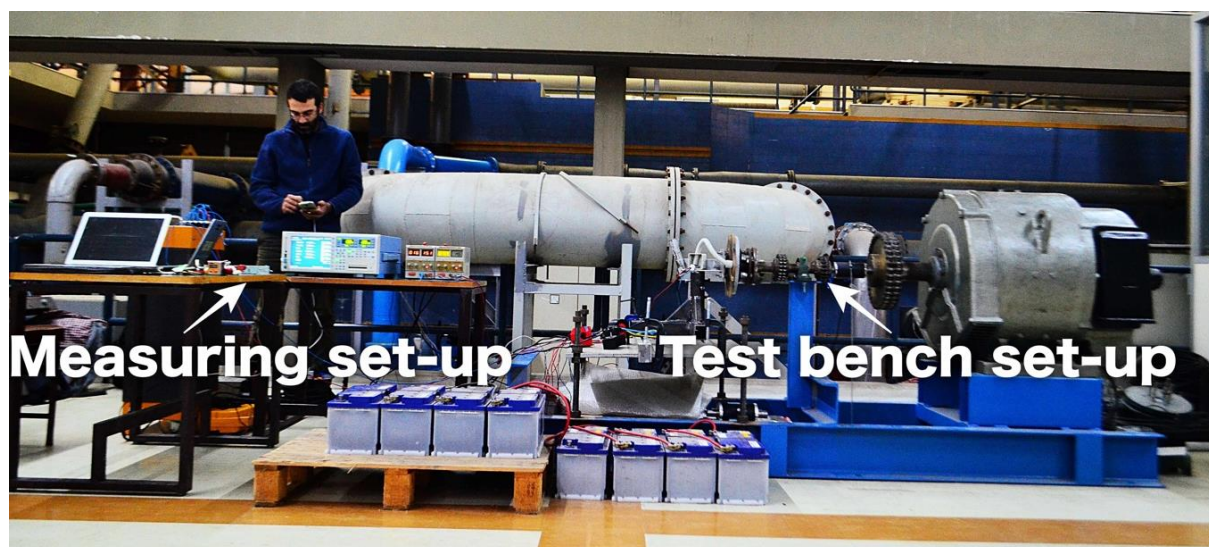
Figure 9: Aligning the shaft of the bench testing set-up
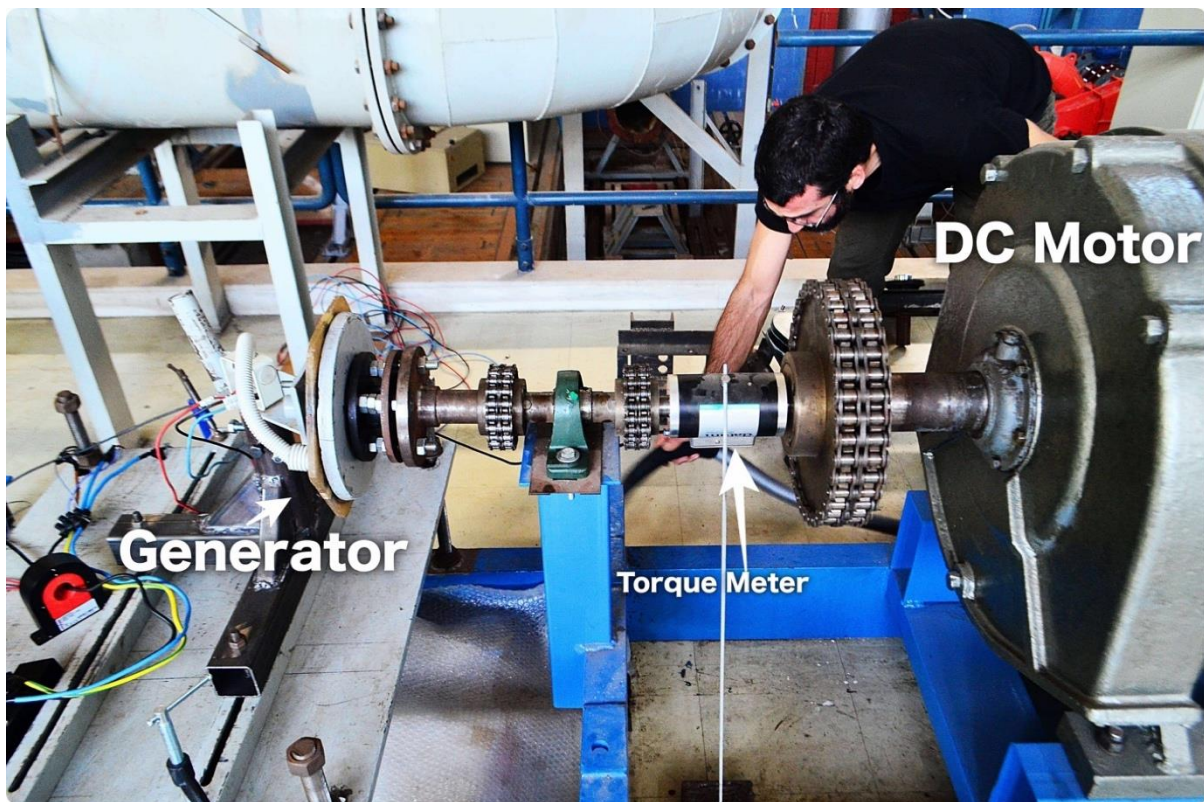
To measure the technical performance of the AFPMG, the following tests were performed and compared with the simulated results which are explained in detail in the following sections of the report.

Stator Resistance	**Open Circuit Voltage**
Battery Load Test	**Generator Losses**

Voltage and frequency readings were recorded using a power analyser while the torque was recorded using the Datum 20Nm torque meter. The rotational speed (rpm) of the generator was calculated using the following formula:

$$P = \frac{120f}{N}$$ Equation 1

P = no. poles (see Table 1: SWT specification table – This is the SWT tested at lab and at test site)

f = frequency (Hz)

N = rotational speed (rpm)

The neutral point was not accessible in the generator. As a result, only line-line measurements could be taken and the following equations were used to convert from line-line and line-neutral measurements:

$$V_{LL} = \sqrt{3}V_{LN} = \frac{V_3}{3}$$ Equation 2

$$I_{LL} = I_{LN} = I_3$$ Equation 3

V = voltage (V)
I= current (A)
LL = line-line
LN = line-neutral
3 = 3-phase

The following equation was used to calculate the apparent power from the recorded line-line/line-neutral voltage and current measurements:

$$S = 3V_{LN}I_{LN} = \sqrt{3}V_{LL}I_{LL}$$ Equation 4

S = apparent power (VA)

5.2.1 Stator Resistance

Figure 10: Schematic of the experimental set up for the DC resistive load test.
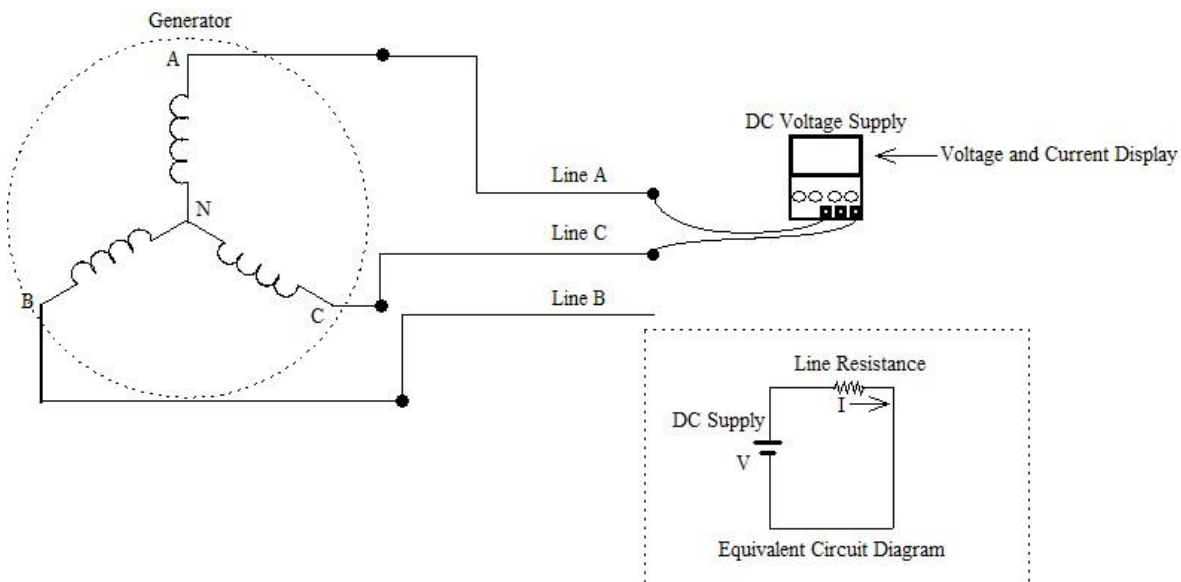
The resistance of the stator governs the amount of power lost internally as heat during operation and therefore has a significant effect on the efficiency of the generator. The coil resistances create an internal heat loss which raises the operating temperature of the stator, which can significantly shorten the life of the component if not kept below acceptable levels.

The resistance of each phase in the stator was calculated by using a variable DC power supply to provide an input voltage and measure the corresponding current, from which resistance could be calculated using Ohm's law. The procedure was then repeated for all 3 phases.

Table 2: Measurement instruments used in the DC resistive load test.

Variable	Measurement device	Measurement type
Voltage and current	Variable DC power supply	Instantaneous

5.2.2 Open Circuit Test

Figure 11: Schematic of the experiment
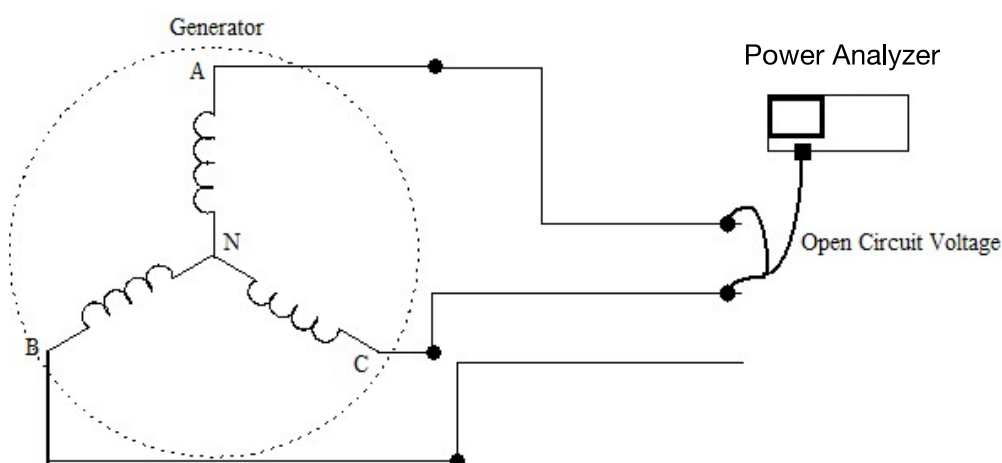
The open-circuit voltage test measures the potential difference produced by each generator at different rotational speeds when no load is present.

The generator terminals were left open circuit so that no current could flow and therefore there is no voltage drop across the stator windings. As a result, in this configuration, there is very little torque in the drive train, that corresponds to the energy losses mainly due to friction and windage in the generator. The driving motor was then operated at different rotational speeds, and the open-circuit voltage and torque were recorded at each speed. The measurement of no-load torque will allow the friction and windage loss from the generator bearing, which is used in the analysis part later to observe the bearing losses through graphical plots at different operating speeds.

Table 3: Measurement instruments used in the open load test.

Variable	Measurement device	Measurement type
AC voltage and frequency	YOKOGAWA, WT3000 Precision Power Analyzer	Instantaneous

5.2.3 Battery load test

Figure 12: Schematic of the battery load test
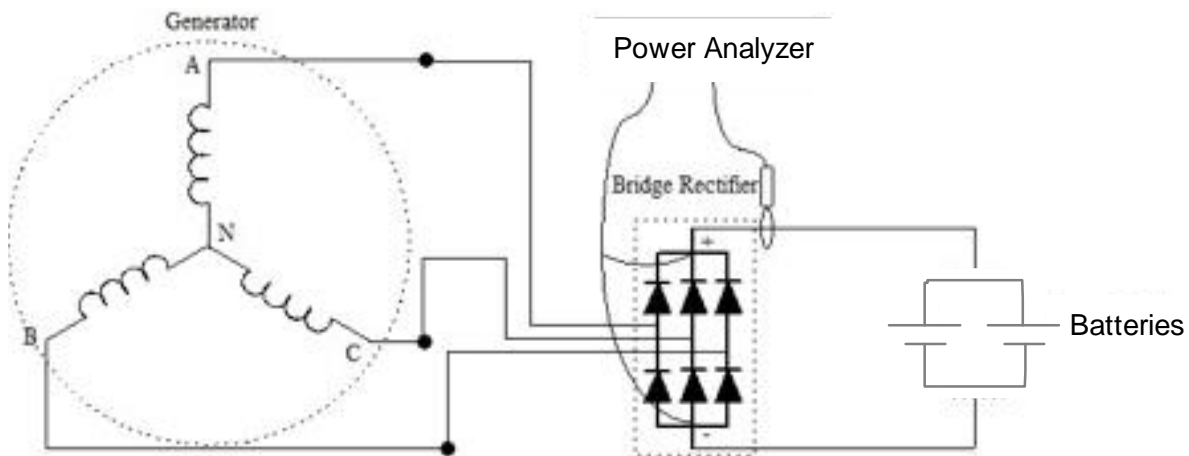
Two sets of 12V, 90Ah batteries are connected in parallel to create a 12V bank, as shown in Figure 12 and Figure 13. The reason for using two batteries in parallel was so that the batteries would sink enough currents to maintain the voltage rise in the acceptable limits compared to using the single 12V battery. The AC voltage and current from the generator are again converted to DC by the three-phase bridge rectifier before passing through the battery terminals. Instead of operating at a constant rotational speed, in this test, the PMG is instead driven at a range of speeds to create a power curve of the machine (power vs rpm). Measurements are taken at intervals of 100rpm up until 700 rpm, when vibration and therefore safety begins to become a concern.

Figure 13: Picture showing the generators connected to the two 12V batteries with electrical measurements taken from the power analyser and the torque meter
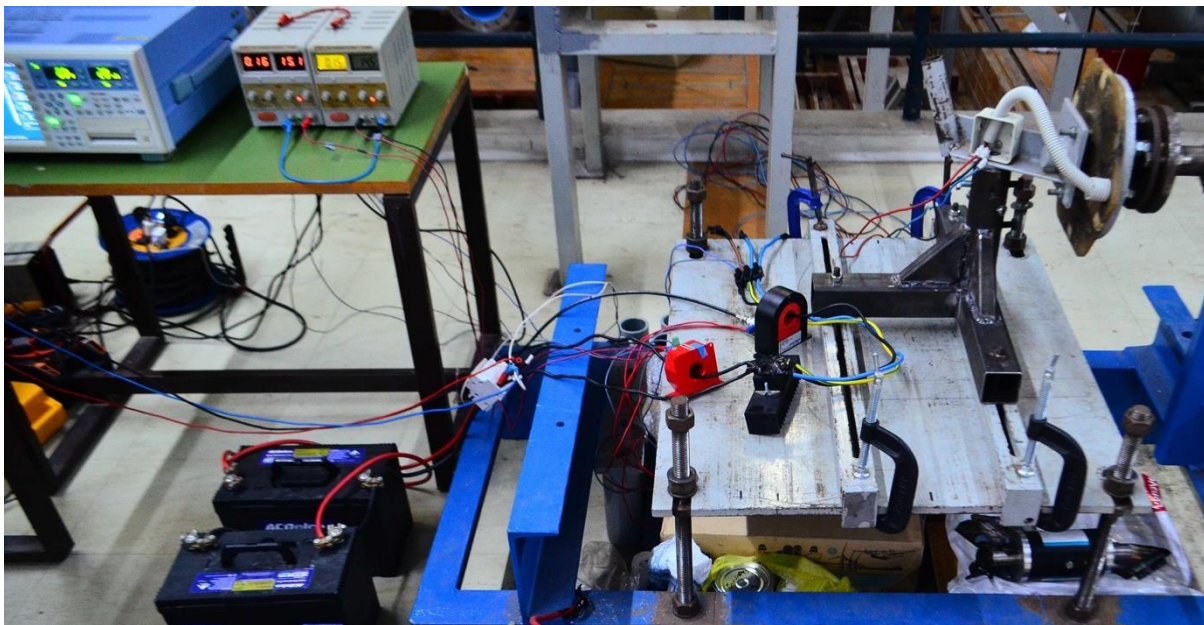
Figure 14: Picture showing the resistive load connected to the batteries to maintain the constant voltage across the battery terminals to maintain the constant battery during higher rotational speeds.
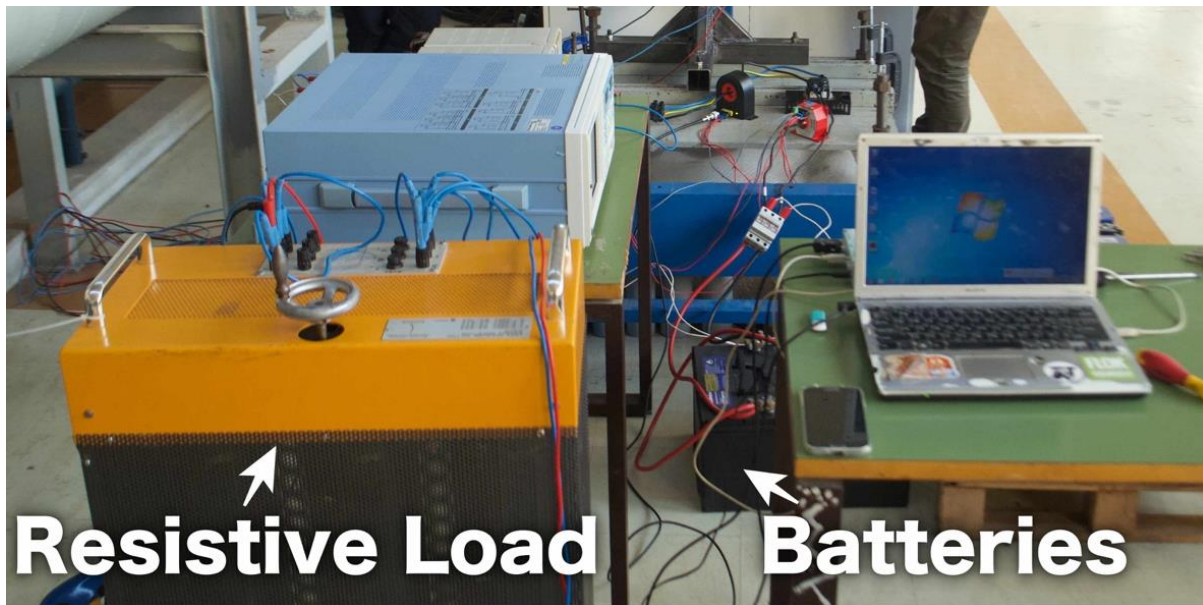
The performance of the generator under load is measured using a three-phase resistive load and a battery load. Data was collected with which to be able to calculate the mechanical and electrical power produced by each generator across a range of operating conditions, which would ultimately allow determination of the torque vs current characteristics of the generator. The distortion in the voltage waveform experienced during each of the loading conditions was also studied.

Mechanical power and AC electrical power are calculated using the following equations:

$$P_{mech} = NT$$ Equation 5
$$P_{AC} = \sqrt{3}V_{LL}I_{AC}$$ Equation 6
$$P_{DC} = V_{DC}I_{DC}$$ Equation 7

P_{mech} = Mechanical Power (W) I_{AC} =Line Current (A) V_{DC} = DC power
N = Rotational speed (RPM) V_{AC} = Line Voltage (V) I_{DC} = DC current
T = Torque (Nm)

Table 4: Measurement instruments used in the battery load test.

Variable	Measurement device	Measurement type
AC/DC voltage/current, frequency, torque, speed	YOKOGAWA, WT3000 Precision Power Analyzer	Instantaneous
Torque and rpm	*Datum* 20Nm torque meter	Transient (averaged)

The harmonics are observed in the oscilloscope in the current and voltage signal when the AFPMG start charging the batteries while the 3-phase bridge rectifier converts the three phase AC to DC. The intensity of dominant harmonics at different operating speeds is observed specially when the current starts flowing into the batteries.

5.2.4 Generator Model

Figure 15 illustrates the power flow diagram from mechanical to electrical between the 3 main components in the test bench comprising of DC motor drive, drive train (with torque meter) and the AFPMG (connected to the load). The DC motor drive is the power source that allows the AFPMG to operate at different rotational speeds. The drive train links the 2 components having the bearing at the centre connected with the torque meter as can be clearly seen in Figure 9.

The ability to measure the losses at various stages of the test bench can be carried out by modelling the AFPMG. The complete electrical model of the AFPMG is shown in Figure 22.

Additionally, the torque meter is capable of measuring up to 20Nm; however, most of the torques measured in this study were below 5Nm. As a result, the lower readings were known to be particularly inaccurate as the torque meter is not designed to accurately measure in this range, where the quantity being measured approaches the resolution of the sensor. Although torque readings were logged and averaged for a number of seconds each time, it was clear that there was significant fluctuation in the readings at low torques, meaning that these results will, therefore, have a high percentage error. This has a knock-on effect on the calculation of mechanical power and efficiency. Therefore, a secondary approach to calculate the machine torque was undertaken, which was the adding losses method for calculating the mechanical power and thus requiring to develop an AFPMG's model first. The alternative approach to calculate the mechanical power created the opportunity to differentiate and analyze the measurements from the two different approaches.

The paper published in the Wind Engineering journal was used as reference to follow the testing method through adding losses to calculate the mechanical power [14]. **Equation 5** is used directly to calculate the mechanical power with and without AFPMG where the torque measurements are collected from the torque meter installed in the drive train and the speed derived from the frequency displayed in the power analyser. The method of calculating mechanical power by adding the generator losses (Equation 8) was used in order to visualize the difference in the calculated power using torque meter and calculating the generator internal losses.

The total mechanical power (P_{mech}) in the AFPMG is the sum of AC Power (P_{AC}), Ohmic losses (P_{OL}) and the friction and windage loss represented by Equation 8.

$$\boldsymbol{P_{mech} = P_{AC} + P_{OL} + F\&W}$$ Equation 8

$$P_{OL} = I^2 R_{avg}$$ Equation 9

$$F\&W = N_{nl}T_{nl}$$ Equation 10

F&W = Friction and windage of the generator
P_{OL} = Generator ohmic loss
N_{nl} = No load rotational speed (rpm)
T_{nl} = No load Torque (Nm)

The determination of ohmic losses (*Equation 9*) is carried out by using the average resistances as in Table 5 and the line currents measured at different rotational speeds.

The friction and windage losses are the losses occurring in bearing of the AFPMG. This loss at different mechanical speeds were measured by simply running the AFPMG at no load and measuring the torque at respective speeds.

The only torque imposed in the generator at open load is the friction and windage in the bearing of the alternator and the test bench. The no load torque of the AFPMG is characterized by the *Equation 10* [14] calculated by multiplying torque and speed at open load. The measurements were taken during open circuit tests mentioned in 0. Therefore, the losses due to friction and windage is calculated by measuring the open load torque with alternator and without AFPMG. The difference of the torque with and without AFPMG is the friction and windage loss in the AFPMG.

Figure 15 illustrates the occurrence of losses at different sections of the test bench set-up in the ICCS-NTUA laboratory.

Figure 15: Schematic showing the losses at different sections of the test set-up.
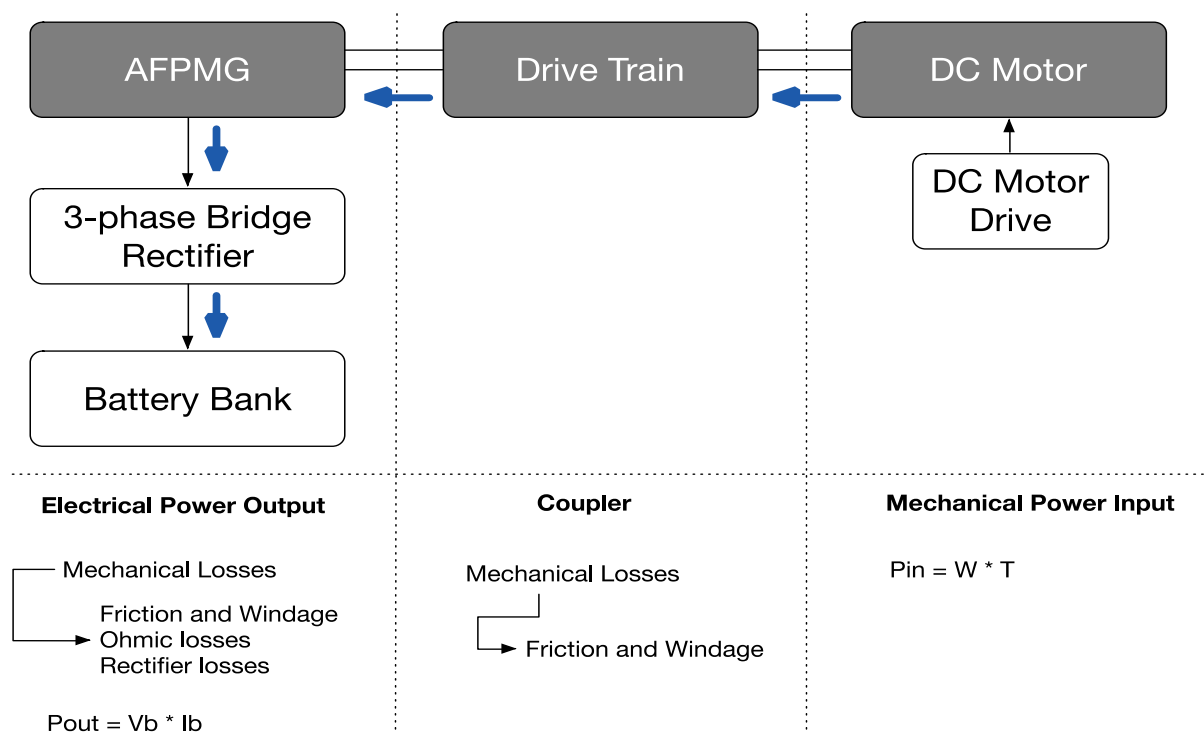
6. Bench Testing Results and Discussion

6.1. Stator Resistance

Table 5 shows the results obtained from the actual line to line resistance measurement carried out with the AFPMG at the lab and the simulated result from the openAFPM.

The AFPMG has only three line out terminals. Therefore, the resistance was measured between the line to line terminals of the generator, as shown in Figure 10. Each of the phases of the AFPMG has two coils in series. Therefore, the average phase resistance is 0.4Ω. The measured phase resistance is very close to the simulation phase resistance, which is 0.34Ω.

The average difference between the measured resistance and the simulation resistance value is 15%. The normal technique used to make the winding coil is by counting each number of turns at the person is making the rounds with the coil. The number of turns may not be accurate for each of the coils, and therefore some difference in resistance is expected with the hand coiling technique.

Table 5: Table showing the measured resistance and simulation resistance between the line terminals of the AFPMG.

Phases	Measured Resistance between line terminals	Resistance from the simulation (3342)
Phase 1 and 2	0.80	0.68
Phase 2 and 3	0.81	0.68
Phase 3 and 1	0.79	0.68
Average	**0.80**	**0.68**

Figure 16: Terminal resistance of the AFPMG from the simulation and the actual measurement
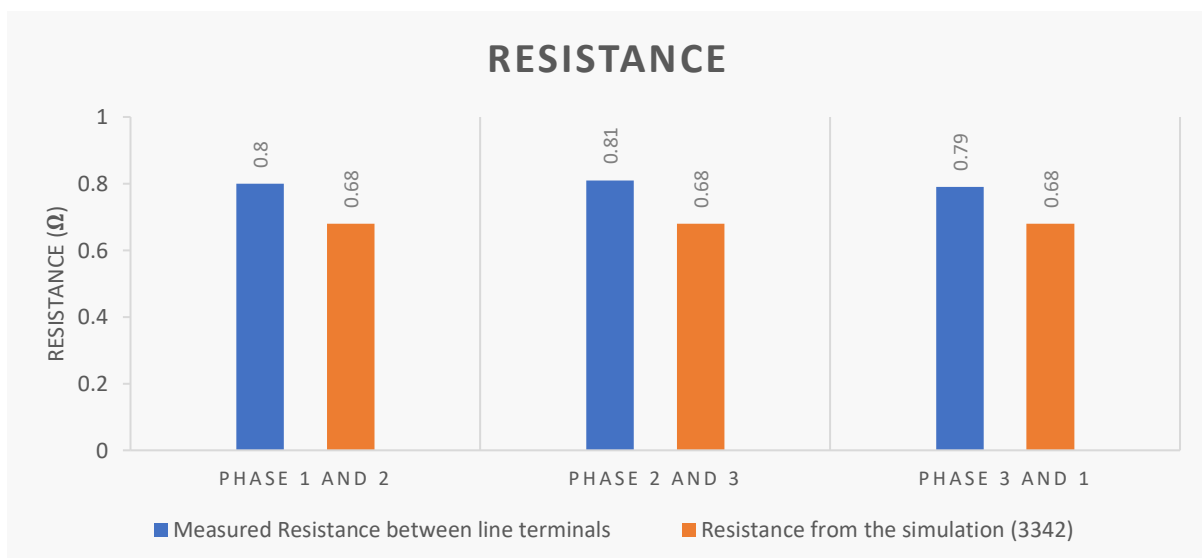
6.2. Open Circuit Tests

The open circuit voltage increases proportionally with the rotational speed. In absence of current, no torque is detected. Figure 17 compares the plot of the measured open circuit voltage from the test bench and the OpenAFPM simulation results as the function of rotational speed. The open circuit voltage plotted in the graph is the terminal line to line voltage between the two phases of the AFPMG.

The simulation results and the measured results are very close to one another for the open circuit voltage test.

Figure 17: The open circuit voltage from the test bench measurement and the OpenAFPM simulation as the function of speed.
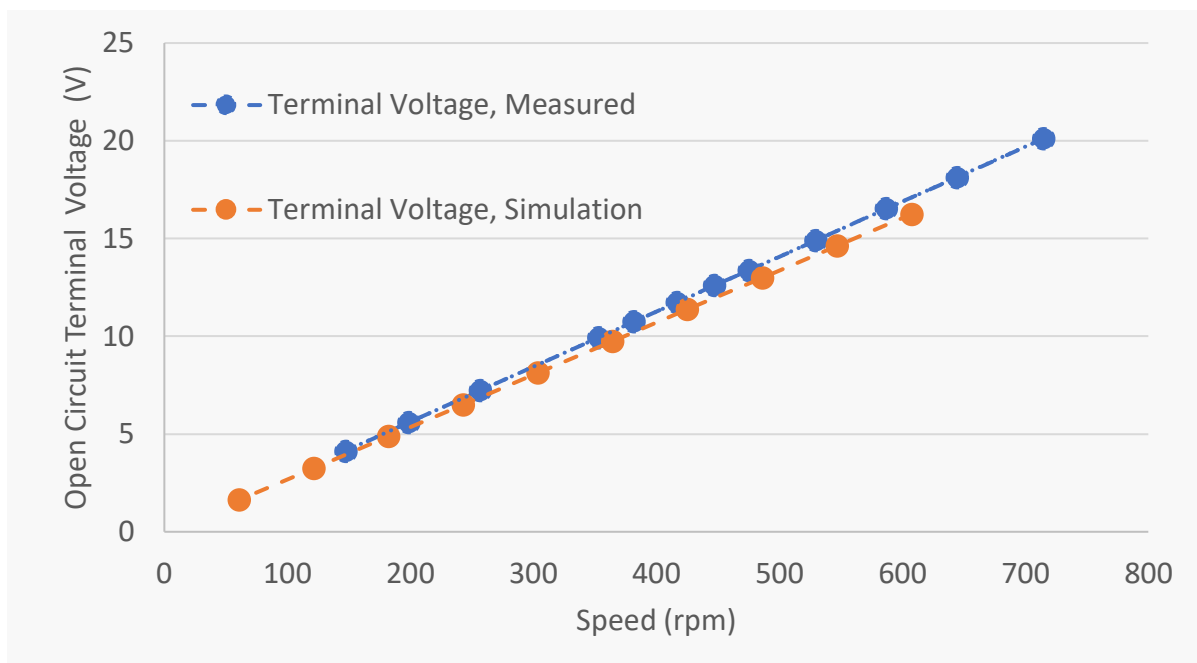
The open circuit line voltage for the AFPMG under test (V_{LL} as in Equation 6) is characterized by the equation below.

$$V_{LL} = 0.0281\,N + 0.0002 \qquad \text{Equation 11}$$

VLL = line to line terminal voltage
N = Rotational speed

6.3. Power and torque with battery load

Batteries eventually culminates as an exact loading for the small wind turbine system. Hence much of the AFPMG tests are focused on the battery load. The increasing current to the battery causes the rise in the battery voltage. To keep the battery voltage constant, the three phase ohmic load is used to dissipate power so as to keep the battery voltage near constant.

The power is plotted for the electrical and mechanical power connected to the battery load. Figure 18 shows the torque-current plot generated from three different approach with the battery connected as the load to the AFPMG.

The torque increases proportionally with current. The relationship between the torque and the current for the AFPMG with battery load is represented by Figure 18.

$T_{(Torquemeter)}$	Indicates the torque measured directly from the torquemeter
$T_{(Adding\ Losses)}$	Indicates the torque calculated by adding losses to the load power (battery)
$T_{(Simulation)}$	Torque measurements from the simulation

The $T_{(Torquemeter)}$ is relatively higher compared to $T_{(Adding\ Losses)}$ and from simulation. The possible reason for the $T_{(Torquemeter)}$ being higher could be because of the extra friction and windage from the bearings of the test bench and the bearings that KAPEG uses for the AFPMG. The open circuit voltage between the simulation and the test measurement could also imply slightly higher torque although minimal. Similarly, the mechanical power (***Equation 8***) using measured torque with battery load displays higher power compared to the mechanical power calculated by adding losses and the simulation.

The battery load torque characteristics is denoted by the equations.

$$\boldsymbol{T(Torquemeter) = 0.4286 * I + 0.5062}$$ Equation 12
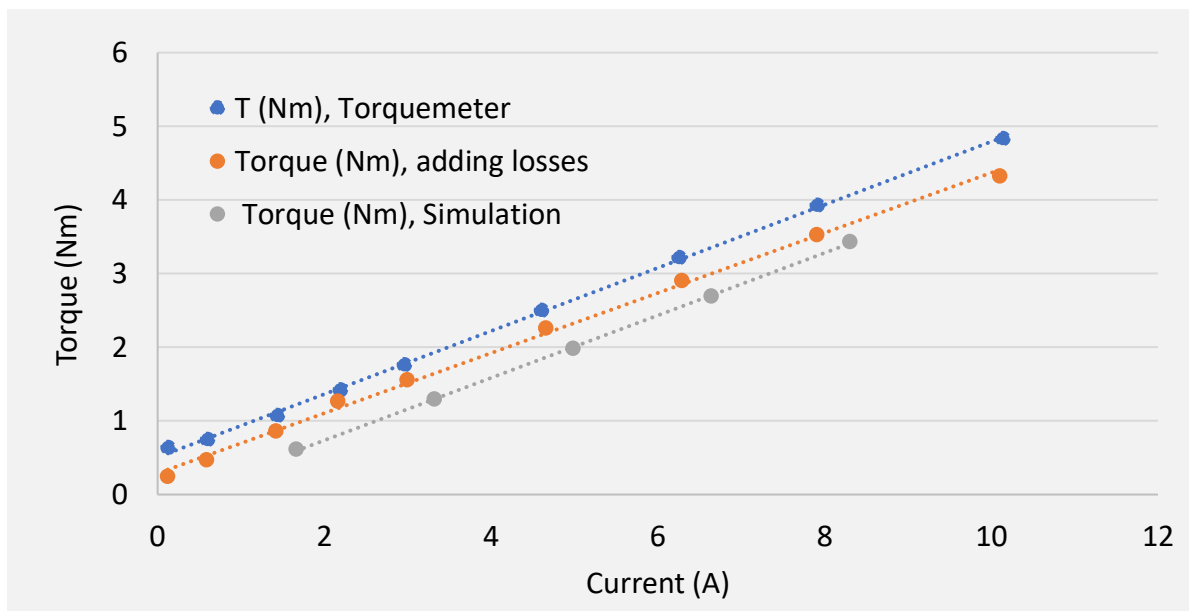$$T(Adding\ losses) = 0.408 * I + 0.2888$$ Equation 13
$$T(Simulation) = 0.424 * I + 0.112$$ Equation 14

I = Line Current

Figure 18:Plot showing the torque calculated from different approaches as the function of line current at different rotational speed.

The electrical power is AC power (Equation 6) using the measured terminal voltages and currents at different rotational speeds.

The generator starts producing power at 350 RPM and starts increasing with the increase in shaft speed. The design cut in speed for the generator is 300 rpm using the openAFPM simulation tool with the difference of 50rpm.

The electrical power consumed by the 12V batteries both seen from the measurements from the test bench and from the simulation results is very close to each other as can be seen in Figure 19.

The mechanical power is calculated from three approaches as mentioned earlier in the report. The mechanical power is comprised of the different losses in the AFPMG. The major losses are incorporated in the calculation which are copper loss and friction and windage loss. The mechanical power calculated directly from the torquemeter, by adding losses and from the simulation is shown in Figure 20 for the purpose of comparative analysis. Figure 20 demonstrates that the mechanical power plot between the power calculated by adding losses and the simulation results are very close to one another while that power calculated from the torquemeter is a bit higher than the other two plots. This distinction may be generated because of some additional torque imposed by the bearings of the test bench.

Figure 19: Battery Load electrical power between the simulation and the actual measurements.
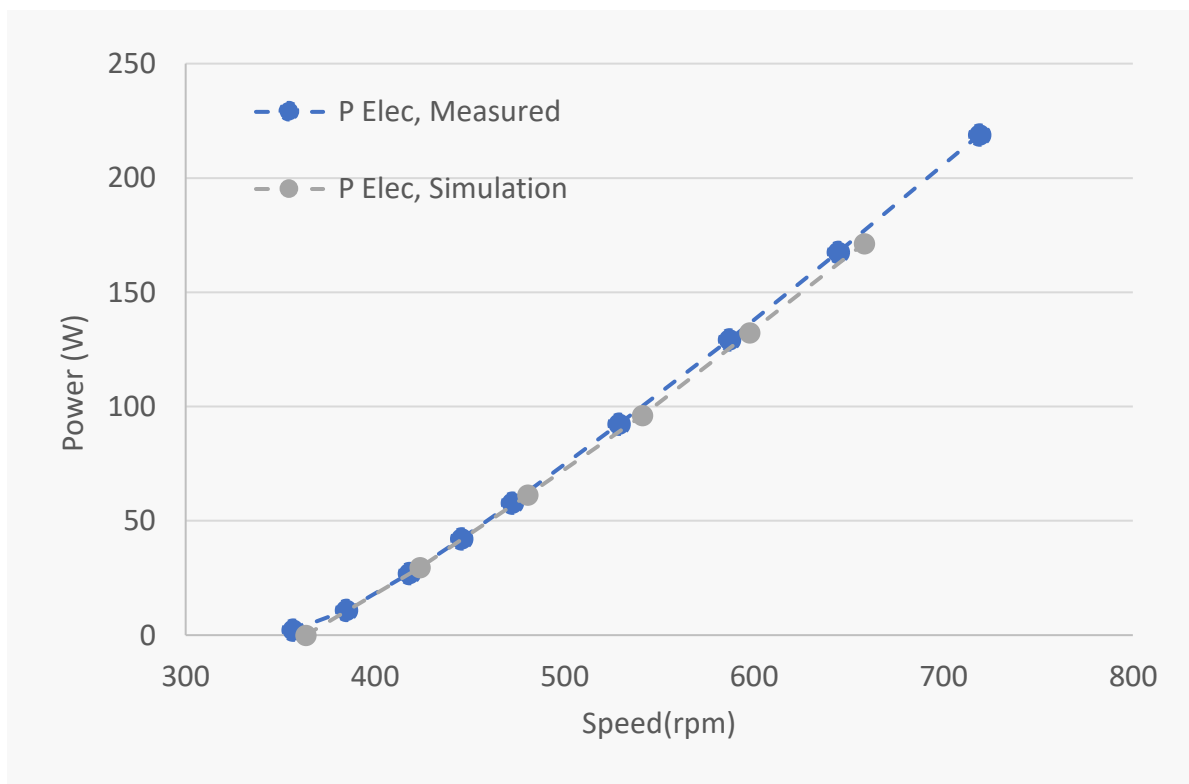
As the torque current characteristics between the simulation and the measured results is significantly close, it is expected that the electrical power would also follow the same as apparent from Figure 19.

The test bench measurements of the AFPMG's electrical power with constant battery voltage load is characterized by equation 15.

$$P(Ac) = 0.6078 * N - 224.65$$ Equation 15

I = Line Current, N = Speed

Figure 20: Mechanical Power comparison between the measurements from torque meter, adding losses and simulation.
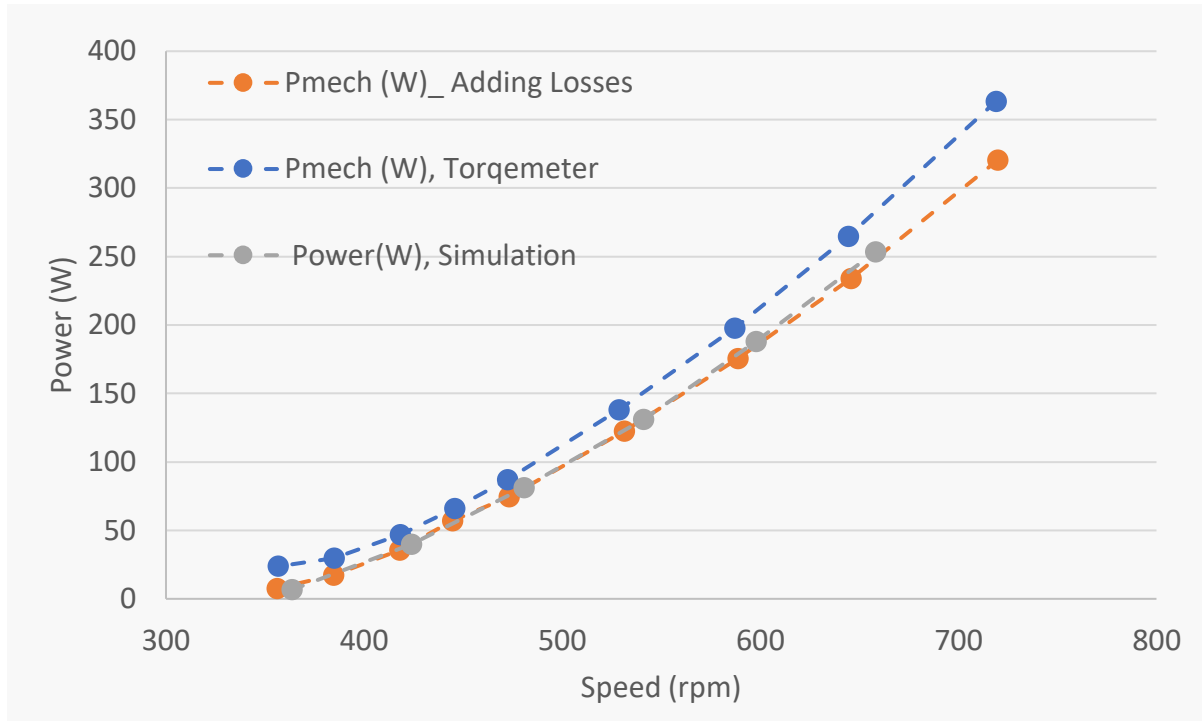
Figure 21: Calculated mechanical power (torque meter) vs speed; The mechanical power calculated by adding losses vs speed; Electrical power vs speed

6.4. Generator Model

Generally, it is not possible to place a torque meter at the top of the tower in the installation site where the turbine is mounted. Therefore, the performance for the wind turbine blades is calculated with the results of the tests carried out in the laboratory. The electrical model of the generator is required to calculate the losses that occurs at different rotating speeds. These losses are copper losses which is the function of the generator impendence and the friction and windage loss.

The complete electrical model of the AFPMG is shown in figure22.

Figure 22: Complete electrical model of the AFPMG
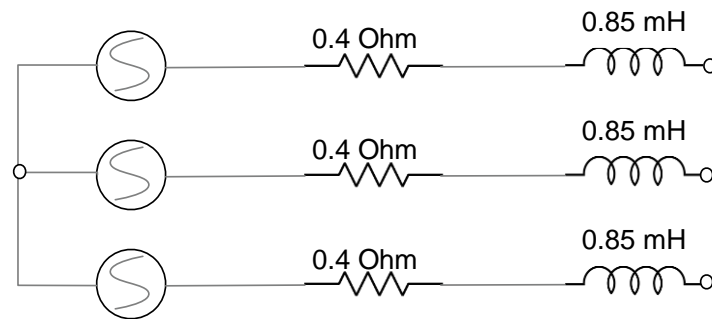
The torque transducer produces measurements with the friction and windage of the generator along with the bearing of the test bench set-up. This can be seen in Figure 8. From a shaft torque transducer, the friction and windage were measured with and without the turbine generator the difference being the friction and windage of the generator (Tfw, eqn. 1). Without the generator, the torque transducer measures the friction and windage losses of itself and the bearings in the test bench.

$$Tfw = 3 * 10^{-4} * N + 0.043$$ Equation 16

T = Torque

fw = Friction and Windage

N = Rotational speed

The losses (eq12) in addition to the copper loss (I^R) and actual load (battery power) at different speeds produces the mechanical power curve.

Figure 23: Measured torque with and without AFPMG
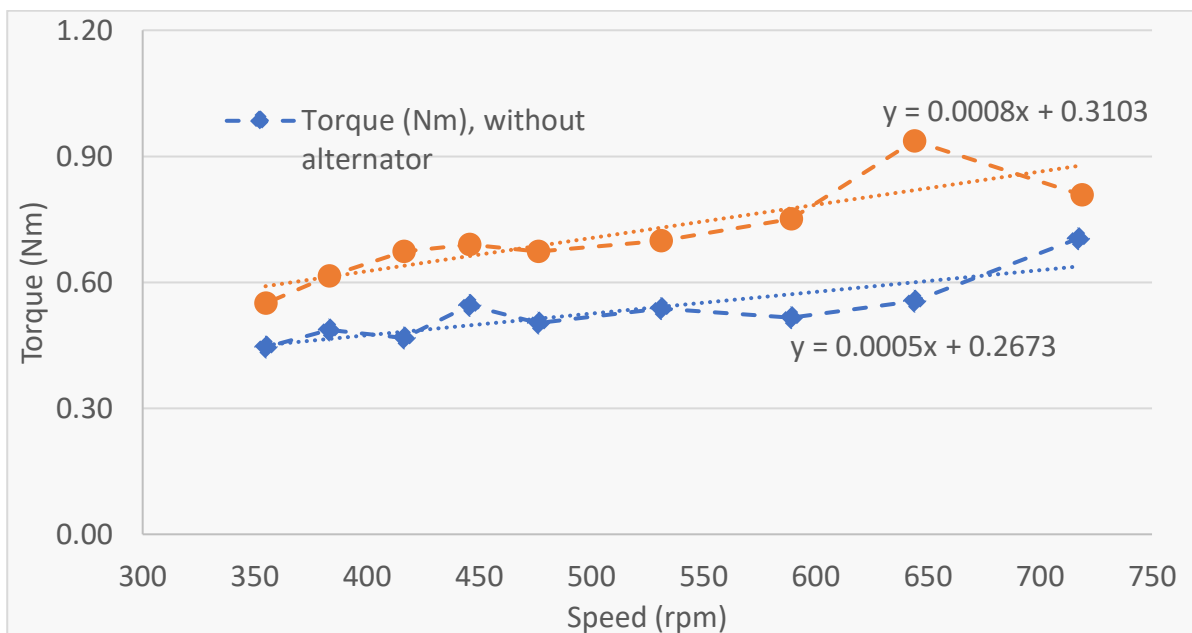
Figure 23 shows the plot of line voltage and currents as the function of rotational speed when the AFPMG is connected to the battery load. The line voltage clearly shows the cutin at approximately

350 rpm when the generator starts charging the batteries with the characteristics of the line currents seen in the same graph.

Figure 24: Graph showing the line voltage and currents with battery load and open load line voltage
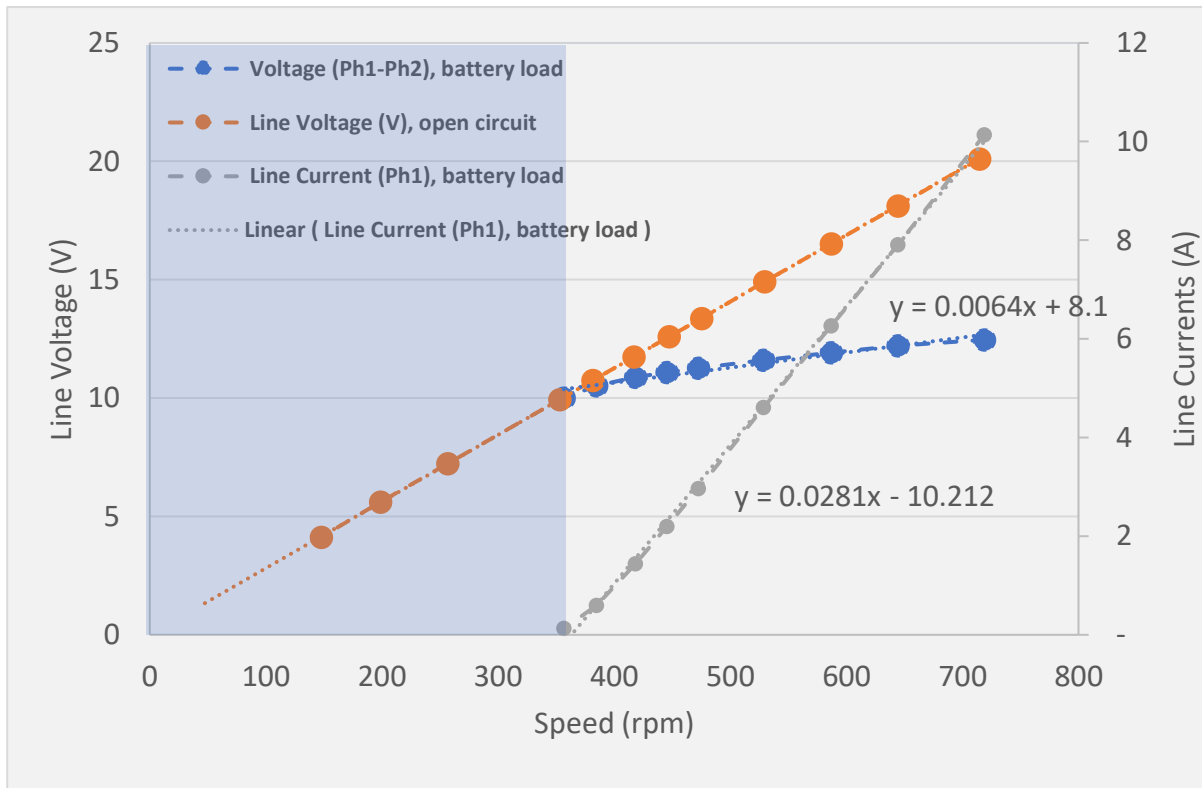
6.4.1 Copper losses

The copper losses occur as an AFPMG's internal loss due to resistance imposed by the copper coils in each of the three phases. The copper losses are also called ohmic losses as characterized by the equation 9 which is the function of the square root of current flowing through the coil resistance.

The measurements from the simulation results are taken from the point to point data labels and transferred to the excel file which is then later compared to the measured test bench results. Figure 25 shows the plot of the copper losses simulation results in the OpenAFPM tool.

The copper losses observed between the simulation and the test bench results is comfortably close to each other as can be seen in Figure 26. The clear difference of the copper loss between the simulation and the test bench could be arising from the difference in phase resistance. Figure 25 shows the plot of the copper loss as the function of rotation speed clipped from the OpenAfpm simulation tool.

Figure 25: Copper loss from the simulation
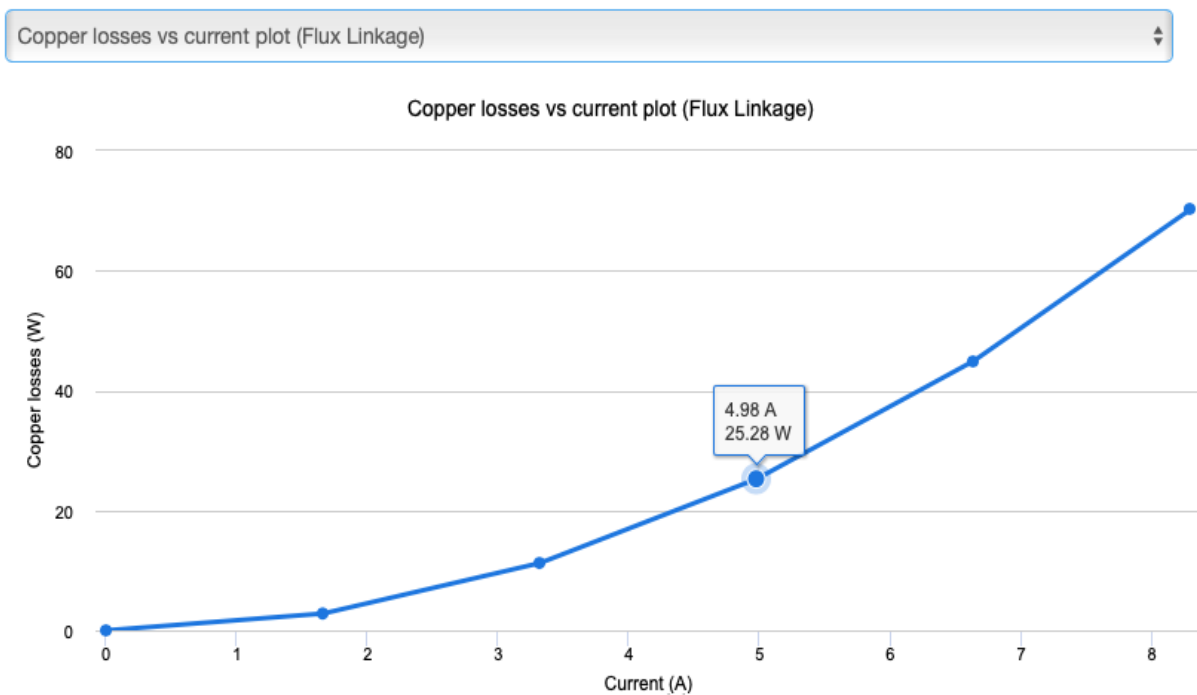
Figure 26: Plot of the comparison in copper losses between the measured values and the simulation results.
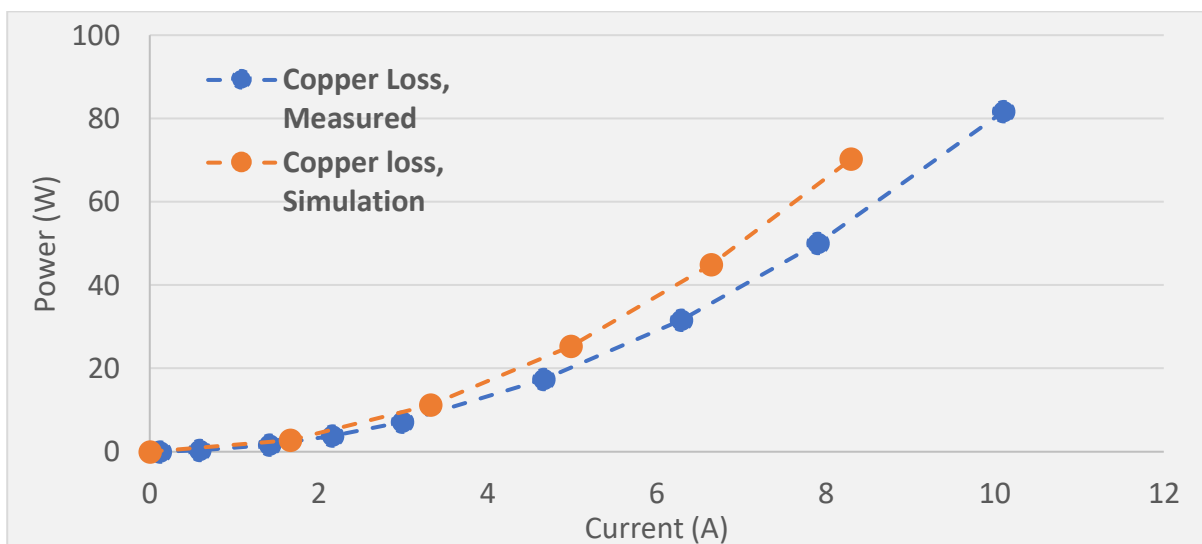
6.4.2 Rotational losses

The rotational losses are the mechanical losses which occurs as frictions in the bearings and the windage due to the air turbulence. These losses are calculated with equation 10 which generates torque values as the function of rotational speed (rpm). The OpenAFPM simulation tool generates the rotational losses as losses in the bearing only.

Figure 27 shows the plot of the rotational losses calculated from the test bench measurements and the rotational losses from the simulation tool. There is an apparent disparity between the two losses

as can be seen in the figure. The disparity is also because of the limitation from the torque meter whose values only starts above 0.5Nm. As the speed increases the losses represented by the calculated results also increases as it carries both the friction and windage losses unlike the values from the simulation.

Figure 27: plot of the generator rotational losses at different operating speed.
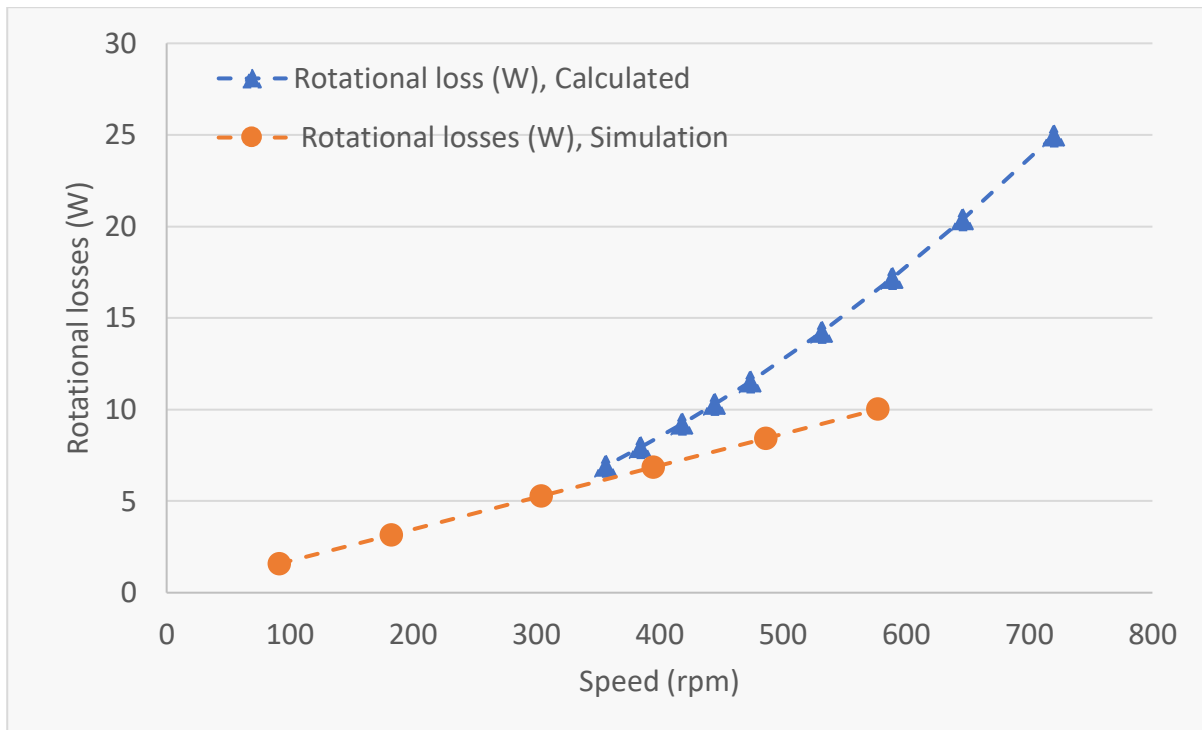
6.4.3 Efficiency

The efficiency of the AFPMG is calculated with the measurements taken from the battery load. For calculating the AFPMG's efficiency, the measurements from the AC side of the generator is taken as is divided by the calculated mechanical power. As the mechanical power is calculated by the three different approaches, the efficiency from the simulation is omitted as it generates the efficiency plots for different fixed current values at various speeds. Therefore, the plots in figure 26 compares the efficiency between the measurements calculated from the torque and from adding losses.

As with the difference between the mechanical power from the simulated results and from the test bench, the efficiency calculated from adding losses is better than the torquemeter measurements. The efficiency peaks at 76% at 440 rpm with adding losses approach while the efficiency calculated directly from the torquemeter peaks at 65% at 465 rpm.

Figure 28: Generator efficiency plot
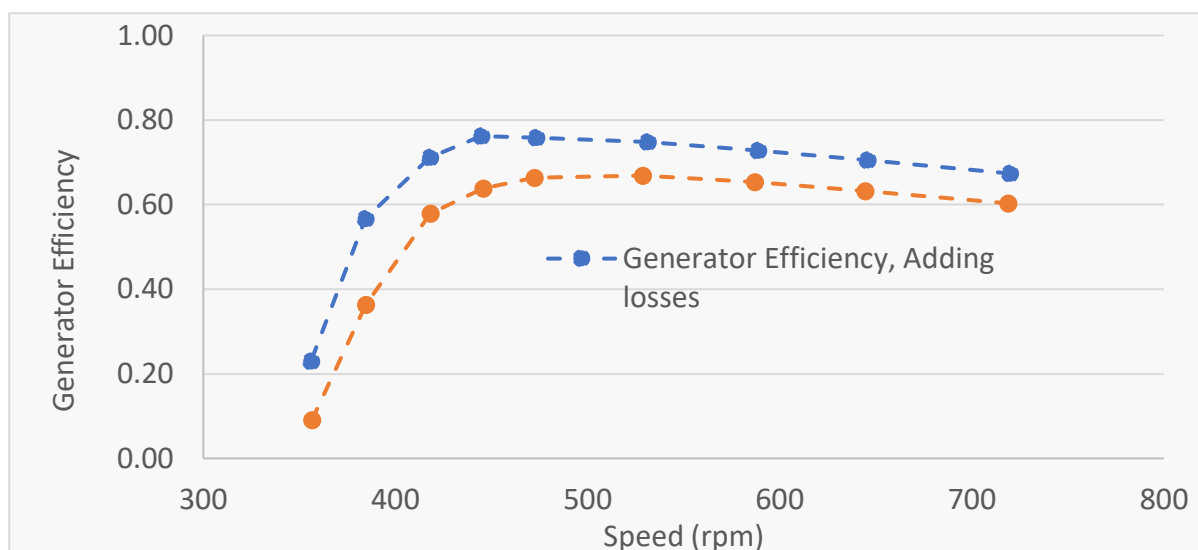
6.4.4 Harmonics at Battery load

With the addition of the bridge rectifier, the harmonics become significant as current increases. The bridge rectifier is necessary to connected batteries as load to the AFPMG. The distortion introduced in the waveform and the harmonic distribution can be observed in Figure 29 when the AFPMG is under battery load. Whilst ohmic losses (leading to heating of the stator) are the main cause of efficiency losses in the generator, the presence of harmonics in the signal wave is also a significant source of losses. Some frequencies can even be detected as audible noise, which manifests itself as a vibration/buzzing of the generator.

Figure 29: Harmonics plot at different speed with AFPMG connected to batteries
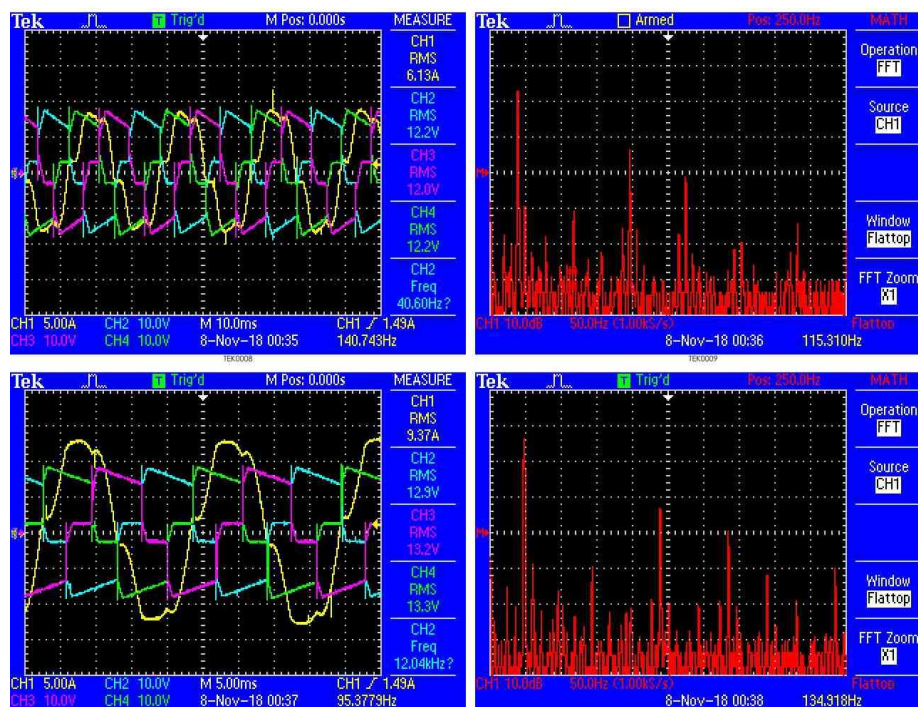
6.4.5 Concluding results - Characterization of the tested AFPMG

Figure 30: Power flow diagram for the AFPMG tested in the lab with battery load maintained at constant voltage.

Pconversion

Pin = T * W

$$T = 0.408 * I + 0.2888$$

Pout = $\sqrt{3}$ V$_{ll}$ * I$_{ac}$

$$P(AC) = 0.6078 * N - 224.65$$

$$Tfw = 3 * 10^{-4} * N + 0.043$$

Friction and Windage Loss
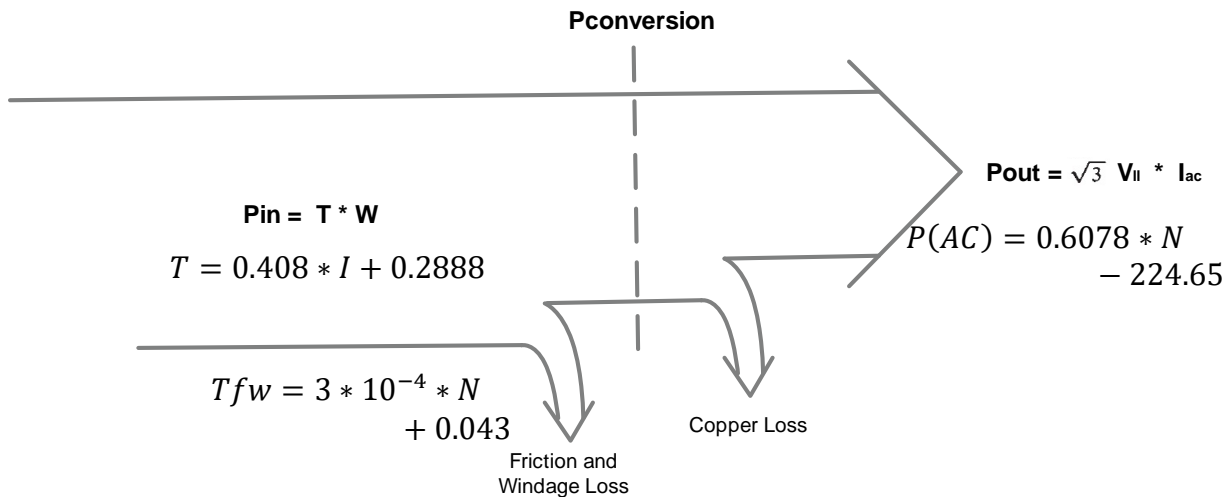
Copper Loss

Figure 30 presents the power flow model of the 12V AFPMG tested in ICCS-NTUA lab. The mechanical power in the shaft of the AFPMG generates electrical power output where the two main losses are considered which are copper loss and friction and windage loss. Other losses such stray loss and core loss are negligible. The AFPMG for small wind turbine machine have coreless stator and the windings have significantly low inductance, hence their impact is not considered in the loss measurements.

The plots from the OpenAFPM simulation tool used for designing the AFPMG tested is compared with the actual measurements extracted from the bench testing results. The correlation between the design tool and the actual measurements will largely be useful to construct the future AFPMG machines of different capacities at KAPEG office with the flexibility is using different available permanent magnets and the copper wires especially.

There is a close resemblance between the torque-speed characteristics of the simulation results and the test bench results (Figure18). The mechanical torque calculated by adding the losses (friction, windage and copper) best matches the simulation results with percentage error of 1%. The mechanical torque taken from the direct measurements from the torque meter compared with the simulation results gives the percentage error of 17%. From the test results, there is a clear indication that the calculated results with adding losses technique significantly matches the simulation.

With close similarly between the torque relationship between the simulation and the adding losses approach, the results plotted and compared for electrical and mechanical power also is very close to one another.

Table 6: Comparison of the power between the test bench results and the simulation

Power comparison	Simulation results	Mechanical Power (Adding Losses)	Mechanical Power (Torquemeter)

| Mechanical power at nominal speed (600rpm) | 228W | 220W | 250W |
| Electrical power at nominal wind speed | 138W | 144W | 144W |

It is quite apparent that the mechanical power calculated using torquemeter incorporates slightly more losses than the one with adding losses. This has a direct effect on the efficiency calculated from these two approaches as seen in Figure 28. The difference of 12% in peak efficiency is observed from the two approaches.

The comparison between the rotational losses from the simulation and the test bench do not produce a discrete differentiation. The rotational losses from the simulation and the test bench measurement cannot be directly compared as the simulation do not consider the windage losses although that may be very little. The rotational loss of 20W is calculated at the maximum allowable shaft speed in the test bench of 720rpm. The copper losses observed between the simulation and the test bench results is comfortably close to each other as can be seen in figure 26. The clear difference of the copper loss between the simulation and the test bench could be arising from the slight difference in phase resistance.

6.5. Evaluation

Although every effort was made to take measurements in the most accurate way possible, the following factors were known to have introduced significant errors:

Poor resolution of torque meter: The torque meter is capable of measuring up to 20Nm; however, most of the torques measured in this study were below 5Nm. As a result, the lower readings were known to be particularly inaccurate as the torque meter is not designed to accurately measure in this range, where the quantity being measured approaches the resolution of the sensor. Although torque readings were logged and averaged for a number of seconds each time, it was clear that there was significant fluctuation in the readings at low torques, meaning that these results will, therefore, have a high percentage error. This has a knock-on effect on the calculation of efficiency, as the torque is used to calculate mechanical (i.e. input) power. Therefore, a secondary approach to calculate the machine torque was undertaken, which was the adding losses method for calculating the mechanical power.

Difficulty in aligning axes*:* The torque measurements was further limited by the difficulty in finding the exact alignment of the axes. This creates additional issues for measuring torque specially for the low torque machine.

Lack of neutral point: in the case of the neodymium generator, line to line voltage was measured just across one particular terminal, as connecting all terminals together at the same time would create a short circuit and continually rewiring would have been very time-consuming.

7. Field testing

7.1. Introduction

During this study, field testing of the SWT generator was carried out by assembling it with the blades, tail and tower and installing it at the NTUA wind turbine test site for monitoring. The performance was monitored live using LabView software, and for recording the instantaneous readings.

7.2. Power curve measurement with data logger

7.2.1 Methodology

7.2.1.1   Experimental set up

The NTUA test site in Rafina allows for outdoor measurements of the power and energy production of household small wind turbines for grid connected and battery charging applications. The facilities of the test site are in accordance to the international standard *IEC 61400-12-1: Power Performance Measurements of Electricity Producing Wind Turbines*, specifically *Annex H,* which refers to small wind turbine testing [15]. This document describes a standardised methodology for measuring the power curve, power coefficient (C_p) and the Annual Energy Production (AEP) of the turbine for different site mean wind speeds. Furthermore, guidance is given on the installation of meteorological and electrical sensors, the analysis of logged data, the presentation of processed data and the estimation of uncertainties.

The NTUA Rafina test site's infrastructure allows for the installation and testing of small wind turbines ranging from 1.2m to 7.6m rotor diameter in off-grid (battery charging) or grid tied operation. The wind turbines are installed at a hub height of 12m on a galvanized metal tower of appropriate diameter and thickness, while the tower is supported by two sets of guys (at 6 and 12m) with four galvanized steel ropes positioned at 90º intervals in each set. The guys are safely anchored to concrete blocks at ground level. The specifications of the steel wire ropes and of the concrete blocks are designed so that the largest turbine under test (7.6m diameter) is able to withstand gusts of up to 40m/s.

Figure 31: Meteorological sensors mounted on the meteorological mast at the NTUA test site in Rafina.

Table 7: Details of the meteorological sensors mounted on the meteorological mast at the NTUA test site in Rafina.

Sensor type	Model / Serial No
Anemometer (control)	NRG-40C
Wind Vane	NRG-200P
Temperature	NRG-110
Pressure	NRG-BP-20
Humidity	NRG-RH-5

Table 8 shows the sensors used to measure electrical data, all of which are placed as close as possible to the battery bank. Three AC voltages and AC currents are logged before the rectifier, with the ability to also measure revolutions per minute (RPM) through the AC signal frequency. After the rectifier, the DC voltage and DC current flowing into the battery bank are recorded for battery charging applications or the DC voltage and DC current flowing through the grid-tie inverter for grid connected applications. In this way the power curve of the turbine can be plotted along with all other relevant data, including losses in the cable connecting the turbine to its load, while the distance of the turbine to the load meets the standards set by *IEC 61400-12-1*. All sensors are calibrated once every year and fulfil the accuracy requirements of *IEC 61400-12-1*.

Table 8: Details of the electrical sensors installed at the NTUA test site in Rafina.

Sensor type	Model / Serial No
Phase R (voltage AC)	LV25-P
Phase S (voltage AC)	LV25-P
Phase T (voltage AC)	LV25-P
Voltage DC	LV25-P

Phase R (current AC)	CSNR151
Phase S (current AC)	CSNR151
Phase T (current AC)	CSNR151
Current DC	CSNR151

Data is logged by *LabView* software and the *National Instruments NI 6225* data acquisition card. Logged data are stored locally on a PC and sent at the end of each day to the *SmartRue* data base in NTUA, with real time remote data observation planned for the near future. The '*Wind Turbine Performance Data Analysis Tool*' developed by *SmartRue*, is a data management tool that allows for in depth analysis of the measurements, either in the per second raw data format or in one minute averages. This enables the user to observe the SWT in small time periods (e.g. in the order of seconds to study gust response), whilst also generating one-minute averages to calculate the power curves and other statistical data according to *IEC 61400-12-1*.

7.2.1.2   Turbine & site

The 2.4m rotor diameter neodymium SWT described in the previous section of testing at the NTUA laboratory was installed and tested in the test site for 6 weeks. It was connected to a 12V battery with a cable run of 77m from tower top to rectifier. A *Morningstar Tristar TS-60* diversion load controller was employed with appropriate wire wound resistors as loads, set with a diversion voltage of 15V.

Figure 32: 1.2m SWT being installed at the test site.

Figure 33: The turbine and meteorological mast installed at the NTUA test site in Rafina.

7.2.1.3 Data logger and sensors

Data is logged every second and labelled with a timestamp in *LabView* through the DAQ card. These values are transferred to the data base at the end of each day. AC currents, voltages and frequencies (for calculation of rpm using the number of poles in each generator) for each of the three phases are measured and recorded. From these values, average currents (MeanCurrent) and average voltages (MeanVoltage) are calculated, which are multiplied together to give electrical power (Power). The meteorological sensors log wind speed (WindSpeed), wind direction (WindSector), pressure (BarPressure), temperature (Temperature), and humidity (Humidity). From these values the density of air (AirDensity) is calculated.

7.2.1.4 Data processing
7.2.1.4.1 Determination of the measured power curve

The measured power curve is determined by applying the "method of bins" for the normalized in terms of air density data sets, using 0,5 m/s bins and by calculation of the mean values of the normalized wind speed and normalized power output for each wind speed bin according to the Equation 17:

Equation 17

$$V_i = \frac{1}{N_i} \sum_{j=1}^{N_i} V_{n,i,j}$$

$$P_i = \frac{1}{N_i} \sum_{j=1}^{N_i} P_{n,i,j}$$

V_i = normalized and averaged wind speed in bin i
$V_{n,i,j}$ = normalized wind speed of data set j in bin i

P_i = normalized and averaged power output in bin i
$P_{n,i,j}$ = normalized power output of data set j in bin i
N = number of 1 min data sets in bin i

7.3. Field Test Results
7.3.1 Power curve

The power curve shown in Figure 43 is a plot of power (W) vs wind speed (m/s) calculated according to the method of bins described previously. Wind speeds bins range from 2m/s to 15.5 m/s and the bin width has been set to 1m/s. A cut-in wind speed of 3m/s is observed, which is typical for a small wind turbine of this type. The furling system starts operation at 7m/s, where the curve begins to deviate from a typical y = ax3 curve. At 9-10m/s, the furling angle increases to greater than 15º, with power production peaking at 162W at 12m/s. Above this wind speed, power production drops to protect the turbine from overheating at higher, but less common wind speeds.

Figure 34: Power curve for the 1.2m rotor diameter 12V small wind turbine installed at the NTUA test site in Rafina with the 200W neodymium generator.
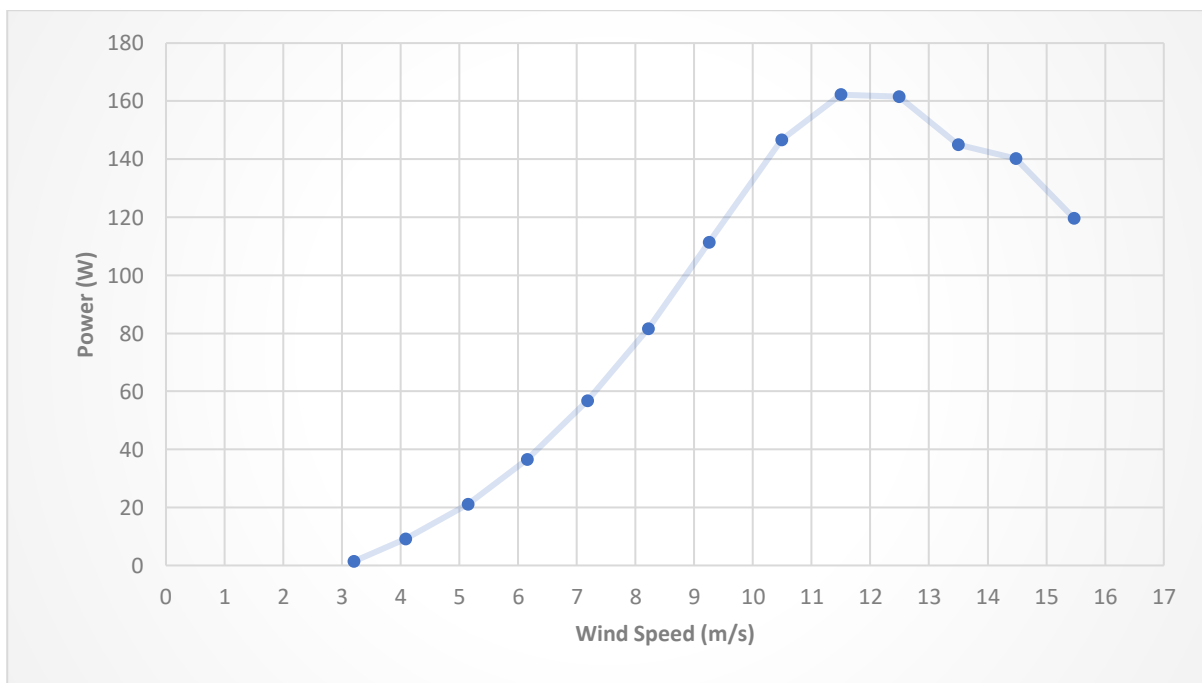
The power coefficient (Cp) plot shown in Figure 44 shows system efficiency (DC electrical power produced at the batteries vs power in the wind) vs wind speed (m/s) and was also calculated using the method of bins. The maximum efficiency is 23% at 6m/s, which is as expected, as the machine is designed to have peak efficiency at the most common wind speed (typically 5m/s for an SWT site).

The peak efficiency is in accordance to which simulation design which is 20%. As wind speeds increase, efficiency drops, meaning that at the rated wind speed of 10m/s, the system efficiency is 20%. This is due to a rapid decline in efficiency after 7.5m/s, which is associated with the action of the furling tail, which is designed to protect the system by reduce the efficiency of the rotor by turning it out of the wind and thus limiting the power production of the system.

Figure 35: SWT efficiency at different wind speed
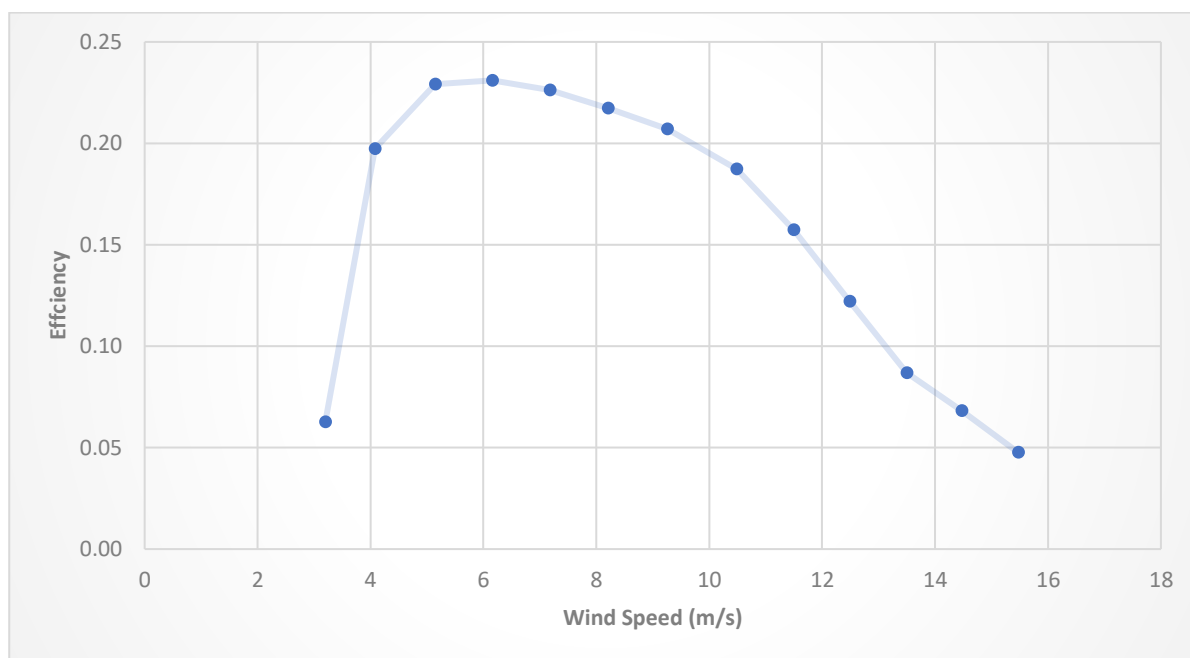
7.4. Field test conclusion

A data logger was used to measure the performance of the 200W neodymium AFPM generator that was previously tested in the laboratory, whilst in normal operation as part of a battery connected wind power system installed at the NTUA Rafina test site according to the international standard *IEC 61400-12-1*. Peak power was measured to be 162W at 12m/s, above which the furling system causes power production to drop in order to protect the turbine from dangerously high winds. The maximum efficiency of 0.23 is reached at 6m/s, whilst at the rated wind speed of 10m/s, the system efficiency drops to 0.2 due to the action of the furling system. On a site with 5m/s mean wind speed, the SWT would be expected to produce 276kWh/year. The cut-in speed with a battery was found to be 359rpm at 3m/s. This closely matches to the simulation design where the system cuts in at 3.2m/s with the rotational speed of the turbine at 348rpm.

Table 9 gives the difference between the simulation results and the calculated results.

Table 9: Comparison table between the simulation tool and the actual tests

Parameters	Open AFPM Simulation Tool	Field Test Results
Cut – in wind speed	3m/s	3.2m/s
Cut - rpm	348rpm	359
Power at nominal wind speed	144W	138W
Rpm at nominal wind speed	607rpm	597rpm
Nominal TSR	3	3.3
Cp peak	0.2	0.23

The field test results extracted from the data logger validates the design conducted from the online simulation tool. The key results from the test site compared with the design concludes that the KAPEG built wind turbine in Nepal performs in the closest range to the design parameters and

therefore provides adequate validation that the simulation tool can be utilized in the future for construction of similar turbine of different capacities with the affordable variations in the generator topologies like magnets and copper wires and bearings

8. **Further work**

The following work is planned to extend the analysis conducted during this study and maximise the usability of the findings:

- The wind turbines tested at ICCS-NTUA would be used to a reference to compare the results with the KAPEG's vehicle test procedure (VTP) in the close future and produce a correlation result. This would provide KAPEG to test the results with other small wind turbines. With KAPEG's work in SWT in the last decade and its existing and upcoming plans, the VTP is the principle activity that KAPEG's will be conducting in the close future.
- The compared results between the simulation tool and the bench testing can be used to produce a better SWT designs with the locally available resources. With the aid of the simulation tool, results for the TA project and the VTP test, KAPEG has large flexibility now to adjust the designs as per component availability and suitability. The upcoming SWT installation therefore can be conducted with larger confidence now than before.
- The existing potential market for solar and wind hybrid system is increasing every year and KAPEG intends to work on standardizing the locally constructed wind turbines in collaboration with the Government of Nepal. Some of the preliminary activities has been developed and delivery mechanism for implementing the concept is under progress. National standardization is a complicated process but KAPEG has been developing grounds for this particular project.
- KAPEG envisions to implement the SWT's in larger scale in the offgrid areas of the country mainly targeted for small communities and institutional installations. The next installation is going to be carried out in early 2020 where the technical knowledge gained from the TA project will be largely useful.

9. **Dissemination**

The Alternative Energy Promotion Center (AEPC) is a focal organization in Nepal operating under the Ministry of Population and Environment which is involved in the development of policies, implementation of renewable energy technologies, delivery of subsidies and encouraging the local sector to play an active role in the field of Renewable Energy. KAPEG is one of the qualified organizations under AEPC who is certified to design, manufacture, assess and commission wind turbine systems in Nepal. KAPEG has collaborated with AEPC multiple times in the past years and therefore the knowledge gained from the TA project would be significant to show the validation of KAPEG's locally fabricated SWT in Nepal. KAPEG will produce a short brief of the product detail and disseminate to the key stakeholders in the national context. The local stakeholders are AEPC, local government (wind potential regions), non-governmental organization working with renewable energies and academic institutions. The national dissemination is targeted to be completed by the end of the year 2020.

Being a active member of Wind Empowerment - global network of small wind turbine practitioners, the test report will be put forth in the wensite as a case study for people seeking relevant information on locally constructed wind turbines and their performance results.

10. **Reference**

[1] R. Sharma, R. Sinha, P. Acharya, L. Mishnaevsky Jr., P. Freere. "Comparison of Test Results of Various Available Nepalese Timbers for Small Wind Turbine Applications", Proceeding of 3rd International Conference – Asia Pacific Region (ISESAP-08) and 46th ANZSES Conference 25-28 Nov. 2008, Sydney, Australia.

[2] R. Sinha, P. Acharya, P. Freere, R. Sharma, P. Ghimire, L. Mishnaevsky Jr. "Selection of Nepalese Timber for Small Wind Turbine Blade Construction" Wind Engineering Vol 34, No. 3, 2010, PP 263-276.

[3] P. Ghimire, R. Sharma, C. Lamichhane, P. Freere, R. Sinha, P. Acharya. "Kathmandu Alternative Power and Energy Group: Our Experience in promotion of Low Cost Wind Energy Technology in Nepal. Wind Engineering Vol., No 3, 2010, PP 313-324.

[4] H. Piggott, *A Wind Turbine Recipe Book*. Scoraig, Scotland: Scoraig Wind Electric, 2013.

[5] Nepal Energy Situation. (2016, May 3). Retrieved June 1, 2017, from https://energypedia.info/wiki/Nepal_Energy_Situation

[6] ESMAP, World Bank Group and International Energy Agency, 2017 *"Sustainable Energy for All, Global Tracking Framework 2017"*

[7] Rai, K. (2016, September 4). Renewable Energy Capacity Needs Assessment- Nepal [PDF]. Kathmandu.

[8] P. Freere, C. Lamichhane, G. Shrestha, P. Ghimire, R. Sinha, P. Acharya. "Starting and Technical Business in Nepal" Wind Engineering Vol. 33(2), PP 123-138.

[9] South Asia Sub-Regional Economic Cooperation. (n.d.). Retrieved from http://www.aepc.gov.np/sasec/

[10] Silwal, K. (n.d.). Market Assessment for SWT. Retrieved from https://online.kapeg.com.np/projects/market-assessment-for-swt

[11] Silwal, K. (n.d.). VEHICLE TESTING METHOD. Retrieved July 4, 2017, from https://sites.google.com/kapeg.com.np/kapeg/small-wind-turbine-system/vehicle-testing-method?authuser=0

[12] Small Wind Turbine Blade Performance Measurement and Analysis Through Vehicle Test Procedure. (n.d.). Retrieved from http://windempowerment.org/wp-content/uploads/2015/07/PosterPresentations_KS_VT.pdf

[13] OpenAFPM. (n.d.). Retrieved July 26, 2019, from https://rurerg.net/open-source-platform/software/openafpm/

[14] Freere, P., Sacher, M., Derricott, J., & Hanson, B. (2010). A Low Cost Wind Turbine and Blade Performance. Wind Engineering, 34(3), 289-302. doi:10.1260/0309-524x.34.3.289

[15] IEC, "Wind Turbines," in Part 12-1: Power Performance Measurements of Electricity Producing Wind Turbines, ed, 2005.